Integrated Channel-Aware Scheduling and Packet-Based Predictive Control for Wireless Cloud Control Systems

Pengfei Li, *Member, IEEE*, Yun-Bo Zhao, *Senior Member, IEEE*, and Yu Kang, *Senior Member, IEEE*

Abstract—The scheduling and control of wireless cloud control systems involving multiple independent control systems and a centralized cloud computing platform are investigated. For such systems, the scheduling of the data transmission as well as some particular design of the controller can be equally important. From this observation, we propose a dual channel-aware scheduling strategy under the packet-based model predictive control framework, which integrates a decentralized channel-aware access strategy for each sensor, a centralized access strategy for the controllers, and a packet-based predictive controller to stabilize each control system. First, the decentralized scheduling strategy for each sensor is set in a noncooperative game framework and is then designed with asymptotical convergence. Then, the central scheduler for the controllers takes advantage of a prioritized threshold strategy, which outperforms a random one neglecting the information of the channel gains. Finally, we prove the stability for each system by constructing a new Lyapunov function, and further reveal the dependence of the control system stability on the prediction horizon and successful access probabilities of each sensor and controller. These theoretical results are successfully verified by numerical simulation.

Index Terms—Channel-aware scheduling, model predictive control, noncooperative game, packet-based control.

I. Introduction

WIRELESS networked control systems (WNCSs), that is, control systems with their sensing and control data being transmitted through wireless communication networks, have received increasing attention from both the academia and industry communities in recent years [1]. With the fast development of cloud computing that "centralizes" the computing resources and wireless communication technologies, such as 5G, that enables much reliable data transmission at much lower latency, a technical trend of WNCSs is observed, where the local controller is being moved to the cloud side and the whole system, which may contain a large number of independent control systems, is "cloud" controlled, hence the name "wireless cloud control systems" (WCCSs) [2], [3]. The existing examples of WCCSs can be found in unmanned aerial vehicle supervisory control [4], underwater vehicle navigation [5], etc., and more applications are expected in the near future.

WCCSs have their distinct features compared with conventional WNCSs. First, in any WCCS, it is natural to have multiple independent control systems to be controlled; second, these control systems have to compete for the access of the limited wireless communication channels for data transmission; and finally, all controllers are implemented at the cloud side using the shared cloud computing resources. These distinct features bring unique challenges for the design and analysis of WCCSs. Indeed, individual control systems in WCCSs can be greedy for accessing the communication channel since for each of them more data transmission usually means better control system performance. However, the capacity of the wireless channel is always limited, meaning that the aforementioned needs cannot be satisfied at no cost. Hence, an efficient channel scheduling strategy over the control systems can be vital for successfully designing WCCSs.

Typical scheduling strategies can be either centralized or decentralized, where the former assumes a scheduler/network manager with global knowledge while the latter does not [6]. The centralized scheduling strategies, whether they are periodic [7], [8]; stochastic [9]; state based [10]; channel aware [11]; or control/scheduling co-designed [12]–[14], are collision free, thanks to the available global information. On the other hand, in the absence of the global information, to avoid possible collisions is the key in the design for adaptive event-triggered [15] or channel-aware [16], [17] decentralized scheduling strategies, and the convergence property for such decentralized strategies is usually analyzed by stochastic approximation [15] or Lagrange duality arguments [16]. Neither the classic centralized nor the decentralized scheduling strategies are the ideal candidate for scheduling channel access in WCCSs, due to the fact that the global information in WCCSs is either perfect (as required by centralized scheduling) or nonexistent (as in the case of decentralized scheduling). Indeed, in WCCSs, the system information and the channel conditions of all control systems may be available to the shared

cloud computing platform (cloud side) while only the individual information is available for each sensor. This fact means that for scheduling channel access in WCCSs, centralized approaches for both sensors and controllers can be infeasible while decentralized ones can be too conservative. Moreover, a simple separate design of the decentralized strategy for the sensor and the centralized one for the controller inevitably brings challenges in our endeavor to ensure system stability; hence, the need for a new scheduling strategy that takes consideration of these characteristics and stability requirements of WCCSs.

In this work, we propose a novel dual scheduling strategy under the packet-based predictive control framework. The scheduling strategy incorporates a distributed threshold strategy for sensors and a centralized prioritized threshold strategy for controllers. As a result, the available information at the sensor side and the cloud side is utilized; hence it is suitable for WCCSs. To implement the strategy, one core issue is to assign appropriate access probabilities for each sensor and controller. This is achieved by a joint design with packet-based model predictive control (PBMPC), which optimizes the control performance by considering the state and control constraints on the one hand and actively compensating for the packet losses induced by the scheduling strategy and transmission errors by the packetized transmission on the other.

We also construct a new Lyapunov function that depends on the actual state and the estimated state-based optimal control sequence for the closed-loop stability analysis, since the proposed scheduling and control algorithms bring great challenges for most existing Lyapunov functions, due to the fact that each system is featured by a constrained nonlinear system model and two-channel random packet losses. To be specific: 1) the commonly used quadratic function with linear matrix inequality techniques suitable for linear systems [18], [19] cannot be applied to the nonlinear case; 2) different from the optimal cost function (OCF) form the Lyapunov function in [20]–[24] (where no packet losses or one-channel packet losses are considered), the OCF in this work relies on the estimated state rather than the actual one and, thus, cannot serve as a Lyapunov function; and 3) the Lyapunov function constructed based on an auxiliary optimal control problem in [25] also fails because the analysis builds on the boundedness of consecutive packet losses, but in our work, the time interval between two successful transmissions may be unbounded.

The contributions of this work are summarized as follows.
1) A distributed threshold strategy is designed for each sensor, which is energy efficient in the long run, adaptive to the changes of channel environment, and does not need any strategy update parameters sent from the remote centralized access point [16] or network manager [15].
2) A prioritized threshold strategy is designed for the controllers, which, in contrast to the typical centralized strategies, for example, round robin [8], try-once-discard [26], and random [9], can achieve a higher successful access rate by blocking the transmissions under bad channel condition.

3) A new construction method is provided for the Lyapunov function, bringing two advantages: a) it is capable of handling the two-channel random packet losses compared with the one in [23] and b) it results in more refined stability criteria without using the control input bound compared with the one in [25].
4) The quantitative relationship of the stability to the prediction horizon and the two-channel successful access probabilities (SAPs) is established, which generalizes the result of one-channel packet losses case in [21] and [23].

The remainder of this article is organized as follows. Section II formulates the problem of interest. Section III presents the design of the scheduling strategy and PBMPC scheme. The convergence and stability analysis are demonstrated in Section IV. Section V illustrates the effectiveness of the proposed approach and Section VI concludes this article.

Note that an earlier limited version of this work was reported elsewhere [27], in the absence of the dual scheduling strategy as well as the comprehensive system analysis.

Notations: Throughout this article, $\mathbb{Z}_0$ and $\mathbb{R}_{\geq 0}$ denote the sets of non-negative integers and reals, and $\mathbb{R}^n$ represents the n-dimensional Euclidean space. 0_n and I_n denote the $n \times n$-dimensional zero matrix and identity matrix, respectively. x^{T} and $\|x\|$ denote the transpose and the Euclidean norm of the vector x, respectively. For strategy $x, y \in [0, 1]^n$, $x \leq y$ if $x_i \leq y_i \ \forall i$, and $x < y$ if there exists at least one i such that $x_i < y_i$ and $x_j \leq y_j$ for $j \neq i$. The operator $\mathbb{1}_{\{A\}}$ denotes the indicator function that evaluates to 1 when A is true and 0 otherwise. The floor function is denoted as $\lfloor . \rfloor$, and $\mathbb{P}$ and $\mathbb{E}$ are used for probability and expectation.

II. PROBLEM FORMULATION AND PRELIMINARIES

The considered WCCS is illustrated in Fig. 1, where n independent control systems are remotely controlled by centralized controllers implemented at the cloud computing platform and the information exchanges of both the sensing data and the control data are through wireless channels, which are called the measurement channel (from the sensor to the controller) and the control channel (from the controller to the actuator), respectively. The sensors are power limited.

The plant of the control system i $(i = 1, \ldots, n)$ is described by the following discrete-time nonlinear model:

$$x_i(k + 1) = f_i(x_i(k), u_i(k), w_i(k)), \quad x_i(0) = x_{i0} \tag{1}$$

where $x_i(k) \in \mathbb{R}^{n_i}$ and $u_i(k) \in \mathbb{U}_i \subset \mathbb{R}^{r_i}$ are the state and the control input, respectively; $\mathbb{U}_i$ is a compact set containing origin in its interior; and $w_i(k) \in \mathbb{R}^{m_i}$ is the independent and identically distributed (i.i.d.) disturbance with arbitrary distribution and $\mathbb{E}\{\|w_i\|^s\} \leq d_i^s < \infty$.

Note that any data transmitted through both the measurement and control channels can be lost due to the imperfect wireless communication. Hence, to describe the considered WCCS in its closed-loop form, how the sensing data for each system are transmitted through the measurement channel, and how the control data for each system are transmitted through the control channel, have to be carefully identified.
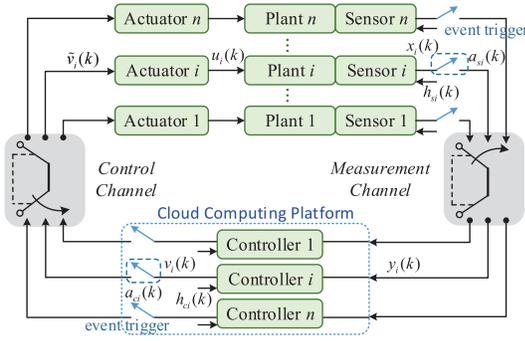
Fig. 1. Illustrating the system structure of wireless cloud control systems, where the controllers of all systems are implemented at the cloud computing platform. h_{si}/h_{ci} (time k is omitted and subscript i means system i) is the channel gain of the measurement/control channel; x_i/y_i is the input/output signal of the measurement channel; $v_i/\tilde{v}_i$ is the input/output signal of the control channel; and u_i is the control input.

For that purpose, we consider the two most common sources of data loss in the considered WCCS. One is the packet collision, that is, the wireless channel can allow but one access at any given time and, hence, multiple accesses at the same time will fail all participants. The other is the transmission error, that is, the transmitted data may not be received error free at the receiver side due to the noise and signal attenuation.

A. Sensing Data Through the Measurement Channel

For any system i at time k, we are interested in the relation between the received data packet at the cloud side, denoted by $y_i(k)$, and the sensing data at the sensor side $x_i(k)$. Note that $y_i(k)$ depends only on $x_i(k)$ at time k but not at any earlier time since no delay is considered in the wireless channel.

First, in our system setting, whether to send $x_i(k)$ is determined by an event trigger as illustrated in Fig. 1, denoted by the following event indicator $a_{si}(k)$ for system i at time k:

$$a_{si}(k) = \begin{cases} 1, & x_i(k) \text{ is transmitted by sensor } i \\ 0, & \text{otherwise.} \end{cases} \tag{2}$$

Second, if $x_i(k)$ is allowed to be sent by the event trigger, it may encounter packet collision, denoted by the following collision indicator $c_{si}(k)$ for system i at time k:

$$c_{si}(k) = \begin{cases} 1, & x_i(k) \text{ is collision-free} \\ 0, & \text{otherwise} \end{cases} \tag{3}$$

which can be determined by the event indicators for all systems, in the following way:

$$c_{si}(k) = a_{si}(k) \prod_{j \neq i, j=1}^{n} \left(1 - a_{sj}(k)\right). \tag{4}$$

Third, even if $x_i(k)$ is allowed to be sent by the event trigger [i.e., $a_{si}(k) = 1$] and is also collision free [i.e., $c_{si}(k) = 1$], it can still be received with error, characterized by the following error indicator $e_{si}(k)$ at time k:

$$e_{si}(k) = \begin{cases} 1, & x_i(k) \text{ is received error-free} \\ 0, & \text{otherwise.} \end{cases} \tag{5}$$

From (2)–(5), we obtain

$$y_i(k) = e_{si}(k)c_{si}(k)a_{si}(k)x_i(k)$$
$$= e_{si}(k)a_{si}(k) \prod_{j \neq i, j=1}^{n} \left(1 - a_{sj}(k)\right)x_i(k). \tag{6}$$

We can conclude that $x_i(k)$ can be successfully received by the controller only if it is allowed to be sent by the event trigger [i.e., $a_{si}(k) = 1$], and its transmission is both collision free [i.e., $c_{si}(k) = 1$] and error free [i.e., $e_{si}(k) = 1$].

Note that (6) is determined by $a_{si}(k)$, $i = 1, \ldots, n$, and $e_{si}(k)$, where the former is further determined by scheduling policies for the sensors, and the latter can be approached by the packet reception probability (PRP) [28], denoted by $P_{si}(h) : [0, \infty) \to [0, 1]$, which is the probability of a packet being received error free and can be explicitly written as

$$P_{si}(h) = \mathbb{P}\{e_{si}(k) = 1 | \zeta_{si}, b_{si}, h_{si}(k) = h\} \tag{7}$$

where $\zeta_{si} \in \mathbb{R}_{\geq 0}$ and $b_{si} \in \mathbb{Z}_0$ are the transmission power of sensor i and the size of the data packet encoding $x_i(k)$, respectively, which are all assumed to be known constants in this work. $h_{si}(k)$ is the channel gain from sensor i to controller i at time step k. We adopt the standard block-fading channel gain model [29], [30] for $h_{si}(k)$, meaning that $\{h_{si}(k), k \geq 0\}$ are i.i.d. random variables with a continuous probability density function (PDF) $o_{si}(h)$, which is available to sensor i before transmitting at time step k. In practice, $h_{si}(k)$ can be estimated by short pilot signals sent from the sensor to the controller, at a sufficiently accurate level [30].

B. Control Data Through the Control Channel

Due to the similarity of the control channel to the measurement channel, the above discussions for measurement channel can be applied to the control channel, with a few modifications. Indeed, for system i at time k, the received control signal $\tilde{v}_i(k)$ is determined in the following way, similar to (6):

$$\tilde{v}_i(k) = e_{ci}(k)a_{ci}(k) \prod_{j \neq i, j=1}^{n} \left(1 - a_{cj}(k)\right)v_i(k) \tag{8}$$

where $v_i(k)$ is the produced control signal by controller i at time k, and all other relevant notions can be similarly defined by simply replacing "s" in the subscript by "c," to denote the change from the measurement channel to the control channel.

C. Scheduling Strategy

In our system setting as depicted in Fig. 1, the data transmission from the sensor to the controller and from the controller to the actuator for each system has to compete with the available communication resources, for which appropriate scheduling strategies are needed. In what follows, we formulate the general form of the scheduling strategy.

Let the scheduling strategy of sensor i at time k be denoted by the time-varying mapping $\pi_{si}^k : \mathcal{H}_{si}(k) \to [0, 1]$, where $\mathcal{H}_{si}(k)$ is the set of all possible channel gain observation history of sensor i until time k. Once the strategy π_{si}^k is determined, then given any $H_{si}(k) \in \mathcal{H}_{si}(k)$, the access probability,

that is, the probability that sensor i is scheduled to transmit at time k ($a_{si}(k) = 1$), is given by

$$\mathbb{P}\{a_{si}(k) = 1 | H_{si}(k)\} = \pi_{si}^k(H_{si}(k)). \tag{9}$$

Similarly, the scheduling strategy for controller i in the cloud computing platform is denoted by $\pi_{ci}^k : \mathcal{H}_c(k) \to [0, 1]$, where $\mathcal{H}_c(k) \triangleq \mathcal{H}_{c1}(k) \times \cdots \times \mathcal{H}_{cn}(k)$ and $\mathcal{H}_{ci}(k)$ is also the set of channel gain observation history. If the observation history is such that $H_c(k) \in \mathcal{H}_c(k)$, the access probability of controller i at time k, that is, the probability of $a_{ci}(k) = 1$, is

$$\mathbb{P}\{a_{ci}(k) = 1 | H_c(k)\} = \pi_{ci}^k(H_c(k)). \tag{10}$$

Since the available channel gains are exploited, the strategies π_{si}^k and π_{ci}^k are called the "channel-aware access strategy" [31]. Observed that the information features at the sensor side [local channel gains $H_{si}(k)$] and at the cloud side [full channel gains $H_c(k)$] are distinct, and therefore, the strategies π_{si}^k and π_{ci}^k should also be distinctly designed.

D. Control Scheme

First, the control law of controller i can be written, in general, as follows:

$$v_i(k) = \bar{v}_i(Y_i(k)) \tag{11}$$

where $Y_i(k) \triangleq \{y_i(0), \ldots, y_i(k)\}$ is the state observation history of controller i, and $\bar{v}_i(.)$ is a causal mapping representing any general controller design method.

Second, the action of actuator i is described by

$$u_i(k) = \tilde{v}_i(\tilde{V}_i(k)) \tag{12}$$

where $\tilde{V}_i(k) \triangleq \{\tilde{v}_i(0), \ldots, \tilde{v}_i(k)\}$ and $\tilde{v}_i(k)$ is the received control signal given in (8), and $\bar{v}_i(.)$ is a mapping from $\tilde{V}_i(k)$ to control constraint set $\mathbb{U}_i$. Note that when the control data are not available, the actuator can implement with the zero-input scheme, hold-input scheme, or other tailored schemes by properly designing $\bar{v}_i$.

E. Problem of Interest

With the above descriptions, we briefly sum up the mechanisms of WCCS running in Fig. 1. At time k, sensor i samples the state $x_i(k)$, which is then sent or not sent, determined by the event trigger with strategy π_{si}^k. Controller i generates the control signal $v_i(k)$ in (11), which is then sent or not sent, determined by the event trigger with strategy π_{ci}^k. Actuator i determines the actual control signal $u_i(k)$ based on (12) and applies it to the plant.

In our system setting, the sensors are power limited and the energy consumption is mainly caused by data transmissions. Hence, the scheduling strategy for the sensors should be energy efficient. Since the transmit power of each sensor ζ_{si} is a constant, we can simply use the following average number of transmissions to represent the energy cost:

$$p_{si} = \limsup_{K \to \infty} \mathbb{E}\left\{ \frac{\sum_{k=0}^{K-1} a_{si}(k)}{K} \right\}. \tag{13}$$

The design objective is to seek for appropriate scheduling strategies π_{si}^k and π_{ci}^k in (9) and (10) and the control scheme $\bar{v}_i$
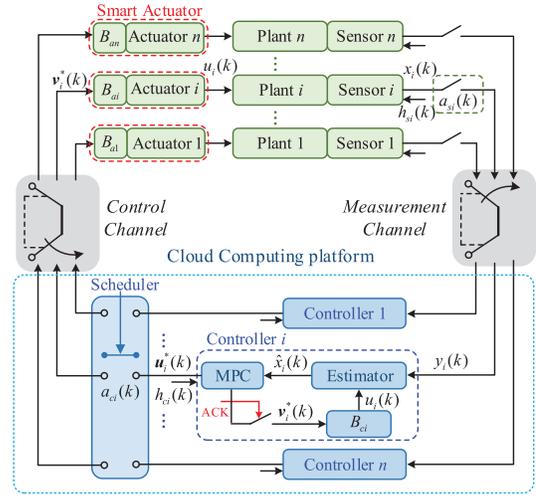
Fig. 2. Dual scheduling PBMPC framework for WCCSs, where B_{ai} and B_{ci} are the buffers for actuator i and controller i, respectively. u_i^* is the output control signal of PBMPC while v_i^* is the received one by the actuator.

and $\bar{v}_i$ in (11) and (12) such that the cost criterion p_{si} in (13) of each sensor is minimized, without violating the stability for each system.

Remark 1: From the stability analysis in what follows, one can observe that the scheduling strategy and control scheme play a coupled role in the closed-loop system stability, which causes the key challenge of the above problem. On the one hand, the feasible scheduling strategy may not exist if the control scheme is not properly designed and, on the other hand, stability may not be guaranteed if the control scheme is designed without considering the interactions with the scheduling strategies. This observation thus motivates our present work on the joint design of both scheduling and control, by carefully building the dependent relationship of the system stability on both the prediction horizon of PBMPC (control scheme) and the two-channel SAPs (scheduling strategy).

III. DUAL SCHEDULING WITH PACKET-BASED MPC

This section proposes the dual scheduling strategy under the PBMPC framework to solve the aforementioned problems, whose system structure is shown in Fig. 2. To implement the control diagram, what remains to design are the decentralized access strategy for each sensor, the centralized selection strategy for the central scheduler, and the PBMPC scheme, which will be detailed in what follows. Note that the strategy to determine two-channel transmissions is called the "dual scheduling strategy" because it consists of both decentralized and centralized ingredients.

Since the channel gain is assumed to be i.i.d. across time, we define the following two channel-aware scheduling strategies independent of the past channel gains, that is, stationary strategy and threshold strategy.

Definition 1: A stationary strategy is a mapping $\pi(h) : \mathbb{R}_{\geq 0} \to [0, 1]$ that depends only on the current channel gain while a threshold strategy is a special type of

stationary strategy with the following particular form:

$$\pi(h) = \mathbb{1}_{\{h \geq \tilde{h}\}}$$

where $\tilde{h}$ is the threshold level.

Remark 2: Note that if a user accesses the channel based on a threshold strategy with threshold $\tilde{h}$, then the average access probability is $p = \int_{\tilde{h}}^{\infty} o(h)dh$, where $o(h)$ is the PDF of channel gain. Conversely, since $o(h)$ is continuous and nonnegative, then p is continuous and nonincreasing with respect to the threshold level $\tilde{h}$. Consequently, given the probability $p \in [0, 1]$, the solution $\tilde{h}$ of the equation $p = \int_{\tilde{h}}^{\infty} o(h)dh$ always exists and can be found by the binary search algorithm.

A. Decentralized Scheduling for Sensors

Each sensor tries to minimize its average power consumption (or equivalently, transmission probability) while meeting the SAP demands by making the transmission decision based on the local channel gains. Since the decision is made independently and transmission interference between sensors exists, the decentralized scheduling problem can be formulated as a noncooperative game with SAP constraints and all sensors being the players. For a random scheduling strategy, each player accesses the channel probabilistically to balance between the access probability and the SAP demand. Denote the stationary strategy for sensor i at time k by $\pi_{si}^k(h_{si})$ (π_{si}^k in short), thus $\boldsymbol{\pi}_s^k = (\pi_{s1}^k, \ldots, \pi_{sn}^k)$ represents the strategy profile of the game under consideration. Let $\boldsymbol{\pi}_{-si}^k$ denote the access strategies of all sensors except sensor i. The superscript k can be neglected if the time is not emphasized.

Given the access strategy profile $\boldsymbol{\pi}_s^k$ and considering (2) as well as (6), the (average) access probability and the SAP of sensor i at each time step k are

$$p_{si}\left(\boldsymbol{\pi}_s^k\right) = \mathbb{P}\{a_{si}(k) = 1\} = \int_0^{\infty} \pi_{si}^k(h)o_{si}(h)dh$$

$$q_{si}\left(\boldsymbol{\pi}_s^k\right) = \mathbb{P}\{e_{si}(k)c_{si}(k)a_{si}(k) = 1\}$$
$$= \int_0^{\infty} \pi_{si}^k(h)o_{si}(h)P_{si}(h)dh \prod_{j \neq i}^n \left(1 - p_{sj}\left(\boldsymbol{\pi}_s^k\right)\right).$$

The outcome of a noncooperative game is characterized as a Nash equilibrium point (NEP) defined below. A basic property of the NEP is that none of the sensors can lower its access probability by unilaterally modifying its strategy.

Definition 2: A strategy profile $\boldsymbol{\pi}_s = (\pi_{s1}, \pi_{s2}, \ldots, \pi_{sn})$ is an NEP if and only if

$$\pi_{si} \in \arg\min_{\hat{\pi}_{si}}\left\{p_{si}\left(\hat{\pi}_{si}, \boldsymbol{\pi}_{-si}\right) : q_{si}\left(\hat{\pi}_{si}, \boldsymbol{\pi}_{-si}\right) \geq \bar{q}_{si}\right\}$$

where $\bar{q}_{si}$ is the preset SAP demand of sensor i.

Lemma 1: The best-response access strategy for each sensor in terms of minimizing the transmission probability while meeting the SAP demand is a threshold strategy.

Proof: See Appendix B. ∎

This lemma confines the optimal strategies of sensors within the set of threshold strategies. Since every threshold strategy can be identified with the access probability, we let $p_{si}(k)$, $\boldsymbol{p}_s(k)$, and $\boldsymbol{p}_{s,-i}(k)$ be the probability representations

of threshold strategy π_{si}^k, $\boldsymbol{\pi}_s^k$, and $\boldsymbol{\pi}_{s,-i}^k$, respectively. Define the following two useful functions for sensor i:

$$H_i(p_{si}) = \int_{\tilde{h}_{si}(p_{si})}^{\infty} o_{si}(h)P_{si}(h)dh \qquad (14)$$

$$q_{si}(p_{si}, \boldsymbol{p}_{s,-i}) = H_i(p_{si}) \prod_{j \neq i}\left(1 - p_{sj}\right) \qquad (15)$$

where $\tilde{h}_{si}(p_{si})$ is the threshold determined by the given access probability p_{si}. $H_i(p_{si})$ represents the SAP of sensor i in the collision-free environment under the threshold strategy and $q_{si}(p_{si}, \boldsymbol{p}_{s,-i})$ is the SAP with collision. Such representations facilitate the following discussions.

To determine and adjust the threshold level of the threshold strategies such that all sensors work at an efficient NEP, we characterize the Nash equilibrium strategy, based on which we then design the strategy update mechanisms.

Lemma 2: A strategy profile $\boldsymbol{p}_s$ is an NEP if and only if it solves a set of equations (equilibrium equations)

$$H_i(p_{si}) \prod_{j \neq i}\left(1 - p_{sj}\right) = \bar{q}_{si}, \ i = 1, \ldots, n. \qquad (16)$$

Proof: According to Definition 2 and the fact that $H_i(p_{si})$ is an increasing function (see Appendix A), an NEP satisfies $p_{si} = \min\{p_{si} : q_{si}(p_{si}, \boldsymbol{p}_{s,-i}) \geq \bar{q}_{si}\}$, where $q_{si}(p_{si}, \boldsymbol{p}_{s,-i})$ is an increasing function with respect to p_{si}. So the solution of the minimization problem also solves (16). ∎

There may not exist an NEP for too severe SAP demands of the sensors. Denote the vector of SAP demands by $\bar{\boldsymbol{q}}_s = \{\bar{q}_{s1}, \ldots, \bar{q}_{sn}\}$, and let Ω represent the set of feasible strategy vectors. As elaborated and proved in [29], when $\bar{\boldsymbol{q}}_s$ lies on the upper boundary set of Ω, there is only one NEP; and when $\bar{\boldsymbol{q}}_s$ is the interior of Ω, there exist two NEPs with one being strictly better than the other. Suppose that $\boldsymbol{p}_s^*$ and $\boldsymbol{p}_s^{\#}$ are both NEPs and $\boldsymbol{p}_s^*$ is the more efficient one, then we have $p_{si}^* < p_{si}^{\#}$, $i = 1, \ldots, n$, and $\sum_{i=1}^n p_{si}^* < 1$.

Noticeably, the Nash-equilibrium strategy is unknown beforehand, so we need to design a mechanism to achieve it. The following two strategy update mechanisms, the best-response dynamic and better-response dynamic, are discussed to answer the question of how each sensor adjusts the access probability to achieve the efficient NEP in a distributed manner.

For the best-response dynamic, each sensor chooses a strategy that minimizes its cost based on the available myopic information (local channel gain). Specifically, since the best response of the sensor i solves the equilibrium (16), we have the following best-response dynamic:

$$p_{si}^{t+1} = \min\left\{H_i^{-1}\left(\frac{\bar{q}_{si}}{\prod_{j \neq i}\left(1 - p_{sj}^t\right)}\right), 1\right\}$$

$$p_{si}(k) = p_{si}^t \quad \forall k \in [Mt, M(t+1)) \qquad (17)$$

where $t = \lfloor k/M \rfloor$ is the iteration count, M is a positive integer representing the strategy update period, and H_i^{-1} is the inverse function of $H_i(p_{si})$. Since the function $H_i(p_{si})$ is continuous and increasing (Appendix A), its inverse function H_i^{-1} exists.

To reduce the computation complexity of H_i^{-1}, the better-response dynamic is adopted. In contrast to the best-response counterpart, the better-response dynamic provides a strategy with performance improvement. The better-response dynamic employed in this article has the following form:

$$p_{si}^{t+1} = \min\left\{\frac{(1-\beta)\bar{q}_{si}}{q_{si}(p_{si}^t, \boldsymbol{p}_{s,-i}^t)}p_{si}^t + \beta p_{si}^t, 1\right\}$$
$$p_{si}(k) = p_{si}^t \quad \forall k \in [Mt, M(t+1)) \tag{18}$$

where $0 \leq \beta < 1$, and $q_{si}(p_{si}^t, \boldsymbol{p}_{s,-i}^t)$ is defined in (15).

The strategy update mechanisms provide the access probabilities for sensors at each time step, and then the corresponding threshold levels can be determined accordingly. Then, the scheduling strategy for each sensor i ($i = 1, \ldots, n$) is

$$\pi_{si}^k(h_{si}(k)) = \mathbb{1}_{\{h_{si}(k) \geq \tilde{h}_{si}(k)\}} \tag{19}$$

where $\tilde{h}_{si}(k)$ is the threshold determined by $p_{si}(k)$.

Remark 3: For the practical implementation of the strategy update mechanisms, including best-response dynamic (17) and better-response dynamic (18), the current SAP $q_{si}(p_{si}^t, \boldsymbol{p}_{s,-i}^t)$ of each sensor i and the idle probability of other sensors $\prod_{j \neq i}(1 - p_{si}^t)$ are needed. $\prod_{j \neq i}(1 - p_{si}^t)$ can be estimated by monitoring the channel utilization [32], and $q_{si}(p_{si}, \boldsymbol{p}_{s,-i})$ can be estimated by counting the number of transmissions and the number of successful transmissions over M time steps based on the acknowledgment signal. But the estimation errors may appear in practical systems, for which we should resort to the notion of ϵ-NEP [33], where each player changes its strategy only if the improved utility is more than ϵ. Note that the strategies of other players are not required, and hence both mechanisms can be implemented in a distributed manner.

B. Selection Strategy for the Central Scheduler

A central scheduler is deployed in the cloud computing platform as shown in Fig. 2. In this section, we design two collision-free randomized selection strategies to choose the appropriate controller at each time step.

We first study the (time invariant) i.i.d. scheduling strategy. Let $\{\sigma(k), k \geq 0\}$ be i.i.d. random variables and $\sigma(k) = i$ means controller i is selected to access the control channel. Note that it is a collision-free strategy, then the access probability and the SAP of controller i are given by

$$p_{ci} = \mathbb{P}\{a_{ci}(k) = 1\} = \mathbb{P}\{\sigma(k) = i\} = \frac{\bar{q}_{ci}}{\sum_{j=1}^n \bar{q}_{cj}} \tag{20}$$

$$q_{ci} = \mathbb{P}\{e_{ci}(k)c_{ci}(k) = 1\} = \frac{\bar{q}_{ci}\int_0^\infty o_{ci}(h)P_{ci}(h)dh}{\sum_{j=1}^n \bar{q}_{cj}} \tag{21}$$

where $\bar{q}_{ci}$ is the SAP demand of controller i satisfying $\bar{q}_{ci} \geq \bar{q}_{si}$. The schedulable assumption is $\int_0^\infty o_{ci}(h)P_{ci}(h)dh \geq \sum_{j=1}^n \bar{q}_{cj}$, which can be easily met and lead to $q_{ci} \geq \bar{q}_{ci}$.

We observe that the i.i.d. scheduling strategy ignores the available full channel gains $\{h_{c1}(k), \ldots, h_{cn}(k)\}$, and the controller with poor channel condition may be selected. To exploit the full channel gains, a threshold strategy is designed. But when multiple controllers obtain the channel gains greater than their thresholds, how should the scheduler make the choice?

To address this problem, we introduce a priority mechanism, where the controller with the highest priority is selected. The priority orders can be set based on the SAP demands, that is, greater demand implies higher priority. We assume index 1 has the highest priority, index 2 has the next priority, and so forth. Without loss of generality, we assume that controller i has priority i, then controller i is activated only if the transmissions of the controllers with higher priorities are forbidden. Once controller i is activated, it checks whether the current channel gain is larger than its threshold or not. If controller i is permitted to transmit, all remaining controllers keep inactivated. Hence, this prioritized threshold strategy uses the full channel gains and is centralized and collision free.

Given the priority orders, we need to determine the threshold for each controller i with priority i. Specifically, we first define the following i.i.d. binary random variable $\theta_i(k)$:

$$\theta_i(k) = \begin{cases} 1, & \text{if controller } i \text{ is activated} \\ 0, & \text{otherwise.} \end{cases}$$

According to the definition of $a_{ci}(k)$ in the previous section, the conditional access probability $\hat{p}_{ci} \triangleq \mathbb{P}\{a_{ci}(k) = 1|\theta_i(k) = 1\}$ for each controller i can be determined recursively

$$\mathbb{P}\{\theta_i(k) = 1\} = \prod_{j=1}^{i-1}(1 - \hat{p}_{cj})$$
$$\hat{p}_{ci} = \frac{p_{ci}}{\prod_{j=1}^{i-1}(1 - \hat{p}_{cj})} \tag{22}$$

where $\prod_{j=1}^0(1 - \hat{p}_{cj}) = 1$ and p_{ci} is defined in (20). Recall that given $\hat{p}_{ci}$ for each controller i, the corresponding threshold $\tilde{h}_{ci}(\hat{p}_{ci})$ ($\tilde{h}_{ci}$ for simplicity) can be determined. Then, a more compact form of the above (time invariant) prioritized threshold strategy can be written as follows, for $i = 2, \ldots, n$:

$$\pi_{c1}(H_c(k)) = \mathbb{1}_{\{h_{c1}(k) \geq \tilde{h}_{c1}\}}$$
$$\pi_{ci}(H_c(k)) = \mathbb{1}_{\{h_{c1}(k) < \tilde{h}_{c1}, \ldots, h_{c,i-1}(k) < \tilde{h}_{c,i-1}, h_{ci}(k) \geq \tilde{h}_{ci}\}}. \tag{23}$$

The above strategy is valid only if $\hat{p}_{ci} \leq 1$, $i = 1, 2, \ldots, n$ (see Theorem 2). Noting that $\mathbb{P}\{a_{ci}(k) = 1|\theta_i(k) = 0\} = 0$, that is, the controller will never transmit any data if it is inactivated, the access probability is $\mathbb{P}\{a_{ci}(k) = 1\} = p_{ci}$, which equals the one given by the i.i.d. strategy in (20). In addition, the SAP of controller i becomes

$$q_{ci}' = \prod_{j=1}^{i-1}(1 - \hat{p}_{cj})\int_{\tilde{h}_{ci}}^\infty o_{ci}(h)P_{ci}(h)dh. \tag{24}$$

Up till now, the dual scheduling strategy, including the decentralized scheduling for sensors and centralized scheduling for controllers, has been designed. One may stress that two important parameters, the SAP demands $\bar{q}_{si}$ and $\bar{q}_{ci}$, have not been determined. These parameters are essential to the design of the control scheme and the stability of the overall system, and will be discussed in Theorem 3 later.

C. PBMPC

In this section, a detailed description of the configuration of PBMPC is presented. Since this is a common configuration for
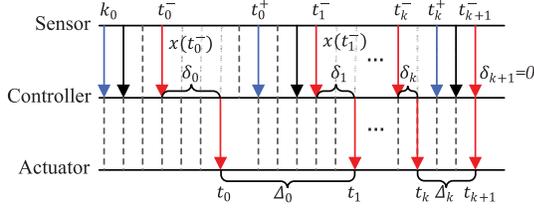
Fig. 3. Example of state/control packet transmissions among sensor, controller, and actuator with possible packet losses.

all systems, the subscript i representing system i is dropped for the ease of presentation.

The basic configuration of PBMPC shown in Fig. 2 is similar to that in [25]. The TCP-like protocol is adopted for both two channels, and an acknowledgment signal, which is useful for scheduling and control, will be sent back to the transmitter.

Under the scheduling strategies of two channels, the SAPs of sensor and controller (denoted by q_s and q_c) are given by (15) and (21) [or (24)], respectively. Fig. 3 shows an example of the packet transmissions over both channels. Denote by $\{t_0, t_1, \ldots\}$ the time instants when the control packet is received by the actuator, and by t_k^- (t_k^+) the last (first) time when the state packet is received by controller *before or at* (*after*) t_k. These notions are essential in the stability analysis.

Controller: The controller consists of three parts: 1) an MPC; 2) a state estimator; and 3) a buffer.

1) The buffer located at the controller side is used to store the received control sequence of the actuator. This can be realized by the ACK signal. Let $\boldsymbol{b}(k)$ denote the content of the buffer at time k and $\boldsymbol{b}(-1) = \boldsymbol{0}$, then we have

$$\boldsymbol{b}(k) = (1 - d_c(k))S\boldsymbol{b}(k-1) + d_c(k)\boldsymbol{u}(k)$$
$$u(k) = e^{\mathrm{T}}\boldsymbol{b}(k) \tag{25}$$

where $d_c(k) \triangleq e_c(k)c_c(k)$, $\boldsymbol{u}(k)$ is the control sequence, $u(k)$ is the control input applied to the plant at time k, and

$$S \triangleq \begin{bmatrix} 0_r & I_r & 0_r & \ldots & 0_r \\ \vdots & \ddots & \ddots & \ddots & \vdots \\ 0_r & \ldots & 0_r & I_r & 0_r \\ 0_r & \ldots & \ldots & 0_r & I_r \\ 0_r & \ldots & \ldots & \ldots & 0_r \end{bmatrix}, \quad e \triangleq \begin{bmatrix} I_r \\ 0_r \\ \vdots \\ 0_r \end{bmatrix}.$$

2) Since the state packet may not be successfully received, we need the following estimator to yield the estimated state:

$$\hat{x}(k) = \begin{cases} x(k), & \text{if } d_s(k) = 1 \\ f(\hat{x}(k-1), u(k-1), 0), & \text{otherwise} \end{cases} \tag{26}$$

where $d_s(k) \triangleq e_s(k)a_s(k)c_s(k)$ and $u(k-1)$ is given by (25). Note that the initial value is set as $\hat{x}(0) = x_0$, which implies that the initial state is available to the controller.

3) The function of MPC is to calculate the control sequence $\boldsymbol{u}(k)$ by solving a constrained optimization problem. If the latest state packet is received by the controller at time k', then the estimated state $\hat{x}(k)$ in (26) can be rewritten as $\hat{x}(k|k')$.

The constrained optimization problem of any one system is then formulated as follows:

$$\min_{\boldsymbol{u}(k)} \quad V_N\big(\hat{x}(k|k'), \boldsymbol{u}(k)\big)$$
$$\text{s.t.} \quad \hat{x}_{j+1}(k|k') = f\big(\hat{x}_j(k|k'), u_j(k), 0\big)$$
$$\hat{x}_0(k|k') = \hat{x}(k|k')$$
$$u_j(k) \in \mathbb{U}, \ j = 0, \ldots, N-1 \tag{27}$$

where $\boldsymbol{u}(k) = [u_0^{\mathrm{T}}(k), \ldots, u_{N-1}^{\mathrm{T}}(k)]^{\mathrm{T}}$, N is the prediction horizon that depends on q_s and q_c, and the objective function is $V_N(\hat{x}(k|k'), \boldsymbol{u}(k)) = \sum_{j=0}^{N-1} l(\hat{x}_j(k|k'), u_j(k)) + F(\hat{x}_N(k|k'))$ with $l(.)$ and $F(.)$ being the stage cost and the terminal cost. Let $\boldsymbol{u}^*(k)$ represent the optimal control sequence of the above optimization problem (27), then the OCF can be written as

$$V_N^*\big(\hat{x}(k|k')\big) = \sum_{j=0}^{N-1} l\big(\hat{x}_j(k|k'), u_j^*(k)\big) + F\big(\hat{x}_N(k|k')\big). \tag{28}$$

Remark 4: Different from the conventional MPC algorithms [20], [21], the above MPC is not performed at every time step. In fact, during the time interval (t_k, t_k^+), no new state packets are received and the latest control packet has been successfully delivered at t_k, and hence the above MPC algorithm will not be carried out. This allows us to lower the computation load and communication load of the control channel. For a more detailed explanation, refer to [25].

Smart Actuator: Similar to buffer 1, the buffer located at the actuator side stores the successfully received control sequence, from which the control input $u(k)$ is selected based on (25). That is, (25) becomes the solution of actuator action in (12).

IV. SYSTEM ANALYSIS

In this section, we analyze the performance of the designed scheduling strategies as well as the stability of each system.

A. Convergence of Strategy Update Mechanisms

For the ease of exposition, we assume that the equilibrium (16) is feasible for whatever changes in the channel environment. Then, the convergence of the strategy update mechanisms can be summarized as follows.

Theorem 1: Let the initial access probabilities be $p_{si}(0) = p_{si}^0 = \bar{q}_{si}$, $i \in \mathcal{I}^B$, where $\mathcal{I}^B$ represents the set of players (sensors). We then have the following conclusions.

1) For a fixed number of players, both the best-response dynamic (17) and the better-response dynamic (18) asymptotically converge to its efficient NEP.
2) Both the best-response dynamic (17) and the better-response dynamic (18) reconverge to a new efficient NEP from its earlier efficient NEP under players joining/leaving the channel.

To prove this theorem, we need the following two lemmas, where Lemma 3 studies the initial condition under which the convergence is ensured and Lemma 4 indicates the changes of the efficient NEP when some players join or leave the channel.

Lemma 3: For the fixed player population case, denote the efficient (better) NEP and the worse NEP by $\boldsymbol{p}_s^*$ and $\boldsymbol{p}_s^\#$, respectively. If we choose the initial access probabilities such that $\bar{\boldsymbol{q}}_s \leq \boldsymbol{p}_s^0 < \boldsymbol{p}_s^\#$, then the best-response dynamic (17) and the better-response dynamic (18) will converge to $\boldsymbol{p}_s^*$.

Proof: First, we show that there exists, for any $\boldsymbol{p}_s^0 < \boldsymbol{p}_s^\#$, new initial access probabilities $\check{\boldsymbol{p}}_s$ that satisfy two conditions: 1) $\boldsymbol{p}_s^0 \leq \check{\boldsymbol{p}}_s < \boldsymbol{p}_s^\#$ and 2) $q_{si}(\check{\boldsymbol{p}}_s) > \bar{q}_{si} \; \forall i \in \mathcal{I}^B$. We set $\check{\boldsymbol{p}}_s = \alpha \boldsymbol{p}_s^* + (1-\alpha)\boldsymbol{p}_s^\#$, where $\alpha \in [0,1)$ is properly chosen such that condition 1) holds. For any i, we have $\log(H_i(\alpha p_{si}^* + (1-\alpha)p_{si}^\#) \prod_{j\neq i}(1 - \alpha p_{sj}^* - (1-\alpha)p_{sj}^\#)) \geq \log(\alpha H_i(p_{si}^*) + (1-\alpha)H_i(p_{si}^\#)) + \sum_{j\neq i}\log(\alpha(1-p_{sj}^*) + (1-\alpha)(1-p_{sj}^\#)) > \alpha \log H_i(p_{si}^*) + (1-\alpha)\log H_i(p_{si}^\#) + \alpha \sum_{j\neq i}\log(1-p_{sj}^*) + (1-\alpha)\sum_{j\neq i}\log(1-p_{sj}^\#) = \log \bar{q}_{si}$.

The above inequalities hold because $H_i(.)$ and $\log(.)$ are strictly concave functions, which further manifest that condition 2) is also satisfied.

Second, we prove that the sequences $\{\bar{\boldsymbol{p}}_s^t\}$ and $\{\underline{\boldsymbol{p}}_s^t\}$ generated by best-response dynamic (or better-response dynamic) with initial condition $\check{\boldsymbol{p}}_s$ and $\bar{\boldsymbol{q}}_s$ converge to the efficient NEP. The results can be proved by introduction.

1) We investigate the convergence of *best-response dynamic* (17) with initial access probabilities $\bar{\boldsymbol{q}}_s$ and $\check{\boldsymbol{p}}_s$, respectively. For the initial probability $\check{\boldsymbol{p}}_s$, from the equilibrium (16), it is trivial to see that $\bar{p}_{si}^0 = \check{p}_{si} \geq p_{si}^*$ and $\bar{p}_{si}^1 = H_i^{-1}(\bar{q}_{si}/[\prod_{j\neq i}(1-\check{p}_{sj})]) \leq H_i^{-1}([H_i(\check{p}_{si})\prod_{j\neq i}(1-\check{p}_{sj})]/[\prod_{j\neq i}(1-\check{p}_{sj})]) = \bar{p}_{si}^0, i \in \mathcal{I}^B$. Now, suppose that the results hold for some $t > 0$, that is, $\bar{\boldsymbol{p}}_s^t \leq \bar{\boldsymbol{p}}_s^{t-1}$ and $\bar{\boldsymbol{p}}_s^t \geq \boldsymbol{p}_s^*$. It remains to show that $\bar{\boldsymbol{p}}_s^{t+1} \leq \bar{\boldsymbol{p}}_s^t$ and $\bar{\boldsymbol{p}}_s^{t+1} \geq \boldsymbol{p}_s^*$. The following inequalities verify the result:

$$p_{si}^* = H_i^{-1}\left(\frac{\bar{q}_{si}}{\prod_{j\neq i}\left(1 - p_{sj}^*\right)}\right) \leq H_i^{-1}\left(\frac{\bar{q}_{si}}{\prod_{j\neq i}\left(1 - \bar{p}_{sj}^t\right)}\right) = \bar{p}_{si}^{t+1}$$
$$\leq H_i^{-1}\left(\frac{\bar{q}_{si}}{\prod_{j\neq i}\left(1 - \bar{p}_{sj}^{t-1}\right)}\right) = \bar{p}_{si}^t. \tag{29}$$

It can then be concluded that strategy profile sequence $\{\bar{\boldsymbol{p}}_s^t\}$ is a decreasing sequence and bounded below by $\boldsymbol{p}_s^*$. Hence, $\bar{\boldsymbol{p}}_s^t$ approaches to a limit, namely, $\bar{\boldsymbol{p}}_s^\infty$. Obviously, $\bar{\boldsymbol{p}}_s^\infty$ satisfies the equilibrium (16), that is, it is also an NEP and $\bar{\boldsymbol{p}}_s^\infty = \boldsymbol{p}_s^*$. For $\bar{\boldsymbol{q}}_s$, we have $\underline{p}_{si}^0 = \bar{q}_{si} \leq H_i^{-1}(\bar{q}_{si}/[\prod_{j\neq i}(1-p_{sj}^*)]) = p_{si}^*$ and $\underline{p}_{si}^1 = H_i^{-1}(\bar{q}_{si}/[\prod_{j\neq i}(1-\underline{p}_{sj}^0)]) \geq \underline{p}_{si}^0$. Suppose that it is true that $\underline{\boldsymbol{p}}_s^t \geq \underline{\boldsymbol{p}}_s^{t-1}$ and $\underline{\boldsymbol{p}}_s^t \geq \boldsymbol{p}_s^*$ for some $t \geq 0$. Similar to the equation in (29), we obtain $\underline{p}_{si}^t \leq \underline{p}_{si}^{t+1} \leq p_{si}^*$, which implies the sequence $\{\underline{\boldsymbol{p}}_s^t\}$ is increasing and bounded upper by $\boldsymbol{p}_s^*$. Then, the limit also exits and is denoted by $\underline{\boldsymbol{p}}_s^\infty$. Similarly, we have $\underline{\boldsymbol{p}}_s^\infty = \boldsymbol{p}_s^*$.

2) The convergence of *better-response dynamic* (18) is studied by a similar method. It can be directly verified that the efficient NEP $\boldsymbol{p}^*$ is also the solution of the following equations $p_{si} = [((1-\beta)\bar{q}_{si})/(q_{si}(p_{si}, \boldsymbol{p}_{s,-i}))]p_{si} + \beta p_{si}, i \in \mathcal{I}^B$, where $q_{si}(p_{si}, \boldsymbol{p}_{s,-i})$ is given in (15). Incorporating fact 4) in Lemma 7 and following the same proof lines, the same conclusion can be drawn.

Finally, we prove that the sequence $\{\boldsymbol{p}_s^t\}$ generated by best-response dynamic (or better-response dynamic) with initial condition $\boldsymbol{p}_s^0$ satisfies

$$\underline{\boldsymbol{p}}_s^t \leq \boldsymbol{p}_s^t \leq \bar{\boldsymbol{p}}_s^t \quad \forall t > 0. \tag{30}$$

We also use the introduction to verify the result. In fact, it is true for $t = 0$. Assume that the inequality holds for any $t > 0$, then for $t+1$, we have

$$p_{si}^{t+1} = H_i^{-1}\left(\frac{\bar{q}_{si}}{\prod_{j\neq i}\left(1 - \underline{p}_{si}^t\right)}\right) \leq H_i^{-1}\left(\frac{\bar{q}_{si}}{\prod_{j\neq i}(1 - p_{si}^t)}\right) = p_{si}^{t+1}$$
$$\leq H_i^{-1}\left(\frac{\bar{q}_{si}}{\prod_{j\neq i}(1 - \bar{p}_{si}^t)}\right) = \bar{p}_{si}^{t+1}$$

for best-response dynamic (17). For better-response dynamic (18), the result can be obtained similarly and thus is omitted. Incorporating the convergence of $\{\underline{\boldsymbol{p}}_s^t\}$ and $\{\bar{\boldsymbol{p}}_s^t\}$ and (30) obtains the convergence of $\{\boldsymbol{p}_s^t\}$. ∎

Lemma 4: Let $\boldsymbol{p}_s^*, \tilde{\boldsymbol{p}}_s^*$, and $\hat{\boldsymbol{p}}_s^*$ represent the efficient NEPs with player set $\mathcal{I}^B$, $\mathcal{I}^B \setminus \mathcal{I}_L$ (removed player set $\mathcal{I}_L$), and $\mathcal{I}^B \cup \mathcal{I}_J$ (new player set $\mathcal{I}_J$), and the worse counterparts are denoted by $\boldsymbol{p}_s^\#, \tilde{\boldsymbol{p}}_s^\#$, and $\hat{\boldsymbol{p}}_s^\#$, respectively. Then, we have $\tilde{p}_{si}^* \leq p_{si}^* \leq \tilde{p}_{si}^\# \; \forall i \in \mathcal{I}^B \setminus \mathcal{I}_L$, and $p_{si}^* \leq \hat{p}_{si}^* \; \forall i \in \mathcal{I}^B$.

Proof: First, we prove the inequality $\tilde{p}_{si}^* \leq p_{si}^* \; \forall i \in \mathcal{I}^B \setminus \mathcal{I}_L$ by the constructive method. Suppose that the strategy profile sequences $\{\boldsymbol{p}_s^t\}$ and $\{\tilde{\boldsymbol{p}}_s^t\}$ are generated by best-response dynamic with initial condition $p_{si}^0 = \tilde{p}_{si}^0 = \bar{q}_{si} \; \forall i \in \mathcal{I}^B \setminus \mathcal{I}_L$ and $p_{si}^0 = \bar{q}_{si} \; \forall i \in \mathcal{I}_L$. Then, from Lemma 3, both two sequences will converge to $\boldsymbol{p}_s^*$ and $\tilde{\boldsymbol{p}}_s^*$, respectively. Now suppose that the inequality $\tilde{p}_{si}^t \leq p_{si}^t \; \forall i \in \mathcal{I}^B \setminus \mathcal{I}_L$ holds for some $t > 0$, then we have

$$p_{si}^{t+1} = H_i^{-1}\left(\frac{\bar{q}_{si}}{\prod_{j\neq i}(1 - p_{si}^t)}\right) \geq H_i^{-1}\left(\frac{\bar{q}_{si}}{\prod_{j\neq i, j\notin \mathcal{I}_L}(1 - p_{si}^t)}\right)$$
$$\geq H_i^{-1}\left(\frac{\bar{q}_{si}}{\prod_{j\neq i, j\notin \mathcal{I}_L}(1 - \tilde{p}_{si}^t)}\right) = \tilde{p}_{si}^{t+1}.$$

Therefore, we have $\tilde{p}_{si}^t \leq p_{si}^t, i \in \mathcal{I}^B \setminus \mathcal{I}_L$ for all $t > 0$. Taking the limit leads to the result. Besides, the inequality $p_{si}^* \leq \hat{p}_{si}^*, i \in \mathcal{I}^B$ can be proved by similar procedures.

The inequalities $p_{si}^* \leq \tilde{p}_{si}^\#, i \in \mathcal{I}^B \setminus \mathcal{I}_L$ are proved by contradiction. Suppose that there exists at least one player $l \in \mathcal{I}^B \setminus \mathcal{I}_L$ such that $p_{sl}^* > \tilde{p}_{sl}^\#$. Note that for any $i \neq l$, $i \in \mathcal{I}^B \setminus \mathcal{I}_L$, we have

$$\frac{\bar{q}_{si}}{\bar{q}_{sl}} = \frac{H_i(p_{si}^*)\prod_{j\neq i}\left(1 - p_{sj}^*\right)}{H_l(p_{sl}^*)\prod_{j\neq l}\left(1 - p_{sj}^*\right)} = \frac{H_i(p_{si}^*)\left(1 - p_{sl}^*\right)}{H_l(p_{sl}^*)\left(1 - p_{si}^*\right)}$$
$$\frac{\bar{q}_{si}}{\bar{q}_{sl}} = \frac{H_i(\tilde{p}_{si}^\#)\left(1 - \tilde{p}_{sl}^\#\right)}{H_l(\tilde{p}_{sl}^\#)\left(1 - \tilde{p}_{si}^\#\right)} > \frac{H_i(\tilde{p}_{si}^\#)\left(1 - p_{sl}^*\right)}{H_l(p_{sl}^*)\left(1 - \tilde{p}_{si}^\#\right)}.$$

With the above equations, we have $[(H_i(p_{si}^*))/(1 - p_{si}^*)] > [(H_i(\tilde{p}_{si}^\#))/(1 - \tilde{p}_{si}^\#)]$, then we can argue that $p_{si}^* > \tilde{p}_{si}^\#$ for all $i \in \mathcal{I}^B \setminus \mathcal{I}_L$.

It should be noted that for any strategy profile $\tilde{\boldsymbol{p}}_s$ satisfying $\tilde{\boldsymbol{p}}_s > \tilde{\boldsymbol{p}}_s^\#$, there exists at least one player i such that $H_i(\tilde{p}_{si})\prod_{j\neq i, j\in \mathcal{I}^B \setminus \mathcal{I}_L}(1 - \tilde{p}_{sj}) < \bar{q}_{si}$. Then, it follows that $H_i(p_{si}^*)\prod_{j\neq i}(1 - p_{sj}^*) < H_i(p_{si}^*)\prod_{j\neq i, j\in \mathcal{I}^B \setminus \mathcal{I}_L}(1 - p_{sj}^*) < \bar{q}_{si}$, which contradicts the fact that $\boldsymbol{p}_s^*$ is an NEP. ∎

Based on the above lemmas, Theorem 1 can be proved.

Proof of Theorem 1: 1) The first assertion is a direct result of Lemma 3 and 2) the second one is proved as follows.

1) When some players leave, we have $\tilde{p}_{si}^* \leq p_{si}^* \leq \tilde{p}_{si}^\#, i \in \mathcal{I}^B \setminus \mathcal{I}_L$, where $\mathcal{I}_L$ is the leaving player set. If the strategy profile $\tilde{p}_{si} = p_{si}^*, i \in \mathcal{I}^B \setminus \mathcal{I}_L$ is the new initial condition, then it follows from Lemma 3 that the best-response (better-response) dynamic will converge to a new efficient NEP $\tilde{\boldsymbol{p}}_s^*$.

2) When some new players join, we have $p_{si}^* \leq \hat{p}_{si}^* \ \forall i \in \mathcal{I}^B$. The new initial strategy profile becomes $\boldsymbol{p}_s = \{\hat{p}_{si}, i \in \mathcal{I}^B \cup \mathcal{I}_J\}$, where $\hat{p}_{si} = p_{si}^*, i \in \mathcal{I}^B$ and $\hat{p}_{si} = \bar{q}_{si}, i \in \mathcal{I}_J$. Then, from Lemma 3, the best-response (better-response) dynamic will reconverge to a new efficient NEP $\hat{\boldsymbol{p}}_s^*$. ∎

Remark 5: Theorem 1 shows that the two strategy update mechanisms (17) and (18) reconverge to a new efficient NEP when channel environment changes. This is an advantage over the strategy in [16] and [17] as the reconvergence may not hold. Moreover, some strategy update parameters, for example, Lagrange multipliers, sent from remote centralized components in [15]–[17] are not needed in our work, which makes the strategy update mechanisms easier to implement.

Remark 6: When $\beta = 0$, the better-response dynamic (18) is similar to the one proposed in [34], where the balanced load condition, that is, $\sum_{j \neq i} [\bar{p}_{sj}/(1 - \bar{p}_{sj})] < 1$ for all $i \in \mathcal{I}^B$, should be met to guarantee the convergence. This condition holds trivially for players with identical SAP demands (symmetric players), but may not hold for asymmetric players [34]. However, since $p_{si}/H_i(p_{si})$ is an increasing function as proved in Appendix A, the convergence can be guaranteed in our context without turning to such extra condition, which removes the application restriction of the better-response dynamic (18).

B. I.I.D. Strategy Versus Prioritized Threshold Strategy

The following theorem validates the prioritized threshold strategy (23) proposed for the central scheduler and reveals its superiority over the i.i.d. scheduling strategy.

Theorem 2: Given the priority order and the access probability p_{ci} of controller i defined in (20). Then, the conditional access probability in (22) satisfies $\hat{p}_{ci} \leq 1$, that is, the scheduling strategy (23) is valid. Furthermore, if the threshold strategy with threshold level $\tilde{h}_{ci}$ is designed for each controller i, it then holds that $q_{ci} \leq q_{ci}'$, where q_{ci}' and q_{ci} are defined in (24) and (21), respectively.

Proof: Indeed, incorporating (20) and (22), we have that

$$\hat{p}_{ci} = \bar{q}_{ci} / \left(\sum_{j=i}^{n} \bar{q}_{cj} \right), i = 1, 2, \ldots, n \qquad (31)$$

which implies that $\hat{p}_{ci} < 1, i < n$ and $\hat{p}_{cn} = 1$. To prove the above equalities, mathematical induction is employed. Let $Q' = \sum_{i=1}^{n} \bar{q}_{ci}$, then $\hat{p}_{c1} = p_{c1} = (\bar{q}_{c1}/Q')$. Suppose that the equality holds for $i = l-1, 2 \leq l \leq n$, then for $i = l$, according to (22) we have

$$\hat{p}_{cl} = \frac{p_{cl}}{\prod_{j=1}^{l-1}(1 - \hat{p}_{cj})} = \frac{\bar{q}_{cl}/Q'}{\frac{\sum_{j=l}^{n} \bar{q}_{cj}}{\sum_{j=l-1}^{n} \bar{q}_{cj}} \prod_{j=1}^{l-2}(1 - \hat{p}_{cj})}$$

$$= \frac{\bar{q}_{cl}/Q'}{\frac{\sum_{j=l}^{n} \bar{q}_{cj}}{\sum_{j=l-1}^{n} \bar{q}_{cj}} \frac{\sum_{j=l-1}^{n} \bar{q}_{cj}}{Q'}} = \frac{\bar{q}_{cl}}{\sum_{j=l}^{n} \bar{q}_{cj}}$$

which completes the proof of $\hat{p}_{ci} \leq 1$.

To verify $q_{ci} \leq q_{ci}'$, we follow the proof similar to that of Lemma 1. Specifically, $\prod_{j=0}^{i-1}(1 - \hat{p}_{cj}) \int_{\tilde{h}_{ci}}^{\infty} o_{ci}(h) P_{ci}(h) dh - q_{ci} = p_{ci}/\hat{p}_{ci} \int_{\tilde{h}_{ci}}^{\infty} o_{ci}(h) P_{ci}(h) dh - p_{ci} \int_0^{\infty} o_{ci}(h) P_{ci}(h) dh = (1/\hat{p}_{ci} - 1) p_{ci} \int_{\tilde{h}_{ci}}^{\infty} o_{ci}(h) P_{ci}(h) dh - p_{ci} \int_0^{\tilde{h}_{ci}} o_{ci}(h) P_{ci}(h) dh \geq p_{ci} P_{ci}[(1/\hat{p}_{ci} - 1)(\tilde{h}_{ci}) \int_{\tilde{h}_{ci}}^{\infty} o_{ci}(h) dh - (\tilde{h}_{ci}) \int_0^{\tilde{h}_{ci}} o_{ci}(h) dh] = p_{ci} P_{ci}(\tilde{h}_{ci})[\hat{p}_{ci}((1/\hat{p}_{ci}) - 1) - (1 - \hat{p}_{ci})] = 0$, where $\int_{\tilde{h}_{ci}}^{\infty} o_{ci}(h) dh = \hat{p}_{ci}$. The proof is then completed. ∎

Remark 7: For controller n (the lowest priority controller), we have $\hat{p}_{cn} = 1$, that is, $\tilde{h}_{cn} = 0$. It means that controller n can access the channel only if the transmissions of all other controllers are not allowed. Hence, the threshold strategy with fixed priority does not bring any improvement for the lowest priority controller. One possible remedy for this drawback is to introduce a changeable priority mechanism, for example, random priority and periodic priority.

C. Stability Analysis

In this section, we analyze the stability of each control system (the subscript i is dropped without any confusion).

The following assumptions and lemmas are necessary to derive the stability conditions.

Assumption 1 [23]: There exist positive constants λ_x, λ_w, λ_l, λ_F, α_l, α_F, and s such that

$$\|f(x, u, w) - f(y, u, 0)\|^s \leq \lambda_x \|x - y\|^s + \lambda_w \|w\|^s$$
$$|l(x, u) - l(y, u)| \leq \lambda_l \|x - y\|^s, \quad l(x, u) \geq \alpha_l \|x\|^s$$
$$|F(x) - F(y)| \leq \lambda_F \|x - y\|^s, \quad F(x) \geq \alpha_F \|x\|^s$$

for all $(x, y, u, w) \in \mathbb{R}^n \times \mathbb{R}^n \times \mathbb{U} \times \mathbb{R}^m$.

Assumption 2 [23]: An auxiliary terminal control law $\kappa : \mathbb{R}^n \to \mathbb{U}$ exists such that for all $x \in \mathbb{R}^n$

$$F(f(x, \kappa(x), 0)) - F(x) + l(x, \kappa(x)) \leq 0. \qquad (32)$$

Assumption 3: There exist positive constants η and $\gamma < \min\{1/(1 - q_s), 1/(1 - q_c)\}$ such that

$$F(f(x, 0, w)) \leq \gamma F(x) + \eta \|w\|^s \qquad (33)$$

for all $x \in \mathbb{R}^n$ and $w \in \mathbb{R}^m$.

The following two lemmas are useful to derive the stability.

Lemma 5 [21]: On the basis of Assumption 2, one obtains

$$l(\hat{x}(k|k'), u_0^*(k)) \leq V_N^*(\hat{x}(k|k')) \leq F(\hat{x}(k|k'))$$

for all $\hat{x}(k|k') \in \mathbb{R}^n$.

Lemma 6 [27]: Define the following two events: $\mathcal{E}_1^k \triangleq \{t_k - t_k^- = \delta_k\}$ and $\mathcal{E}_2^k \triangleq \{t_{k+1} - t_k = \Delta_k\}$ for any $k \geq 0$ with $\delta_k \geq 0$, $\Delta_k > \delta_{k+1} \geq 0$. Then, both the two events $\mathcal{E}_1^{k+1}$ and $\mathcal{E}_2^k$ are independent of event $\mathcal{E}_1^k$, $k \geq 0$. Moreover, if $q_c \neq q_s$, we have $\mathbb{P}\{\mathcal{E}_2^k, \mathcal{E}_1^{k+1}|\mathcal{E}_1^k\} = q_s q_c[q_s(1 - q_s)^{\delta_{k+1}}(1 - q_c)^{\Delta_k} - q_c(1 - q_c)^{\delta_{k+1}}(1 - q_s)^{\Delta_k}]/(q_s - q_c)$ and $\mathbb{P}\{\mathcal{E}_2^k|\mathcal{E}_1^k\} = q_s q_c[(1 - q_c)^{\Delta_k} - (1 - q_s)^{\Delta_k}]/(q_s - q_c)$. If $q_c = q_s$, we have $\mathbb{P}\{\mathcal{E}_2^k, \mathcal{E}_1^{k+1}|\mathcal{E}_1^k\} = q_s^2(1 - q_s)^{\Delta_k + \delta_{k+1} - 1}[(1 - q_s) + q_s(\Delta_k - \delta_{k+1})]$ and $\mathbb{P}\{\mathcal{E}_2^k|\mathcal{E}_1^k\} = q_s^2 \Delta_k(1 - q_s)^{\Delta_k - 1}$. We also obtain

$\mathbb{P}\{\mathcal{E}_1^{k+1}|\mathcal{E}_1^k\} = (1 - q_s)^{\delta_{k+1}}(1 - q_c)^{\delta_{k+1}} - (1 - q_s)^{\delta_{k+1}+1}(1 - q_c)^{\delta_{k+1}+1}$.

With the above preparations, stochastic stability for each system can be established.

Theorem 3: Suppose that Assumptions 2–5 hold, $(1 - q_s)(1 - q_c)\lambda_x < 1$, and the prediction horizon N satisfies that

$$\left[\frac{q_s(1 - q_c)^{N+1}}{1 - (1 - q_c)\gamma} - \frac{q_c(1 - q_s)^{N+1}}{1 - (1 - q_s)\gamma}\right]\frac{\gamma - 1}{q_s - q_c} < \frac{\mu}{1 - \mu}$$
$$q_s \neq q_c$$

$$\frac{Nq_s(1 - \gamma + q_s\gamma) + \left(1 - (1 - q_s)^2\gamma\right)}{(1 - \gamma + q_s\gamma)^2/(\gamma - 1)(1 - q_s)^N} < \frac{\mu}{1 - \mu}$$
$$q_s = q_c$$

(34)

where $\mu \triangleq \inf_{x,u}(l(x, u)/F(x))$. Then, there exist positive constants c_1 and c_2 and $\rho \in (0, 1)$ such that for any $\tau \in [t_k, t_k + \Delta_k - 1]$, $k \in \mathbb{Z}_0$, it holds that

$$\mathbb{E}\{\|x(\tau)\|^s\} \leq c_1(1 - \rho)^k\|x_0\|^s + c_2 d^s \quad (35)$$

and for any $\tau \in [0, t_0 - 1]$, (35) still holds with $k = 0$.

Proof: We first introduce some notations for simplicity. Let $\boldsymbol{u}^*(t_0) = \{u_0^*(t_0), \ldots, u_{N-1}^*(t_0)\}$ be the optimal control sequence obtained by solving the constrained optimization problem at time t_0. The corresponding optimal predictive state sequence is $\{\hat{x}(t_0|t_0^-), \hat{x}_1^*(t_0|t_0^-), \ldots, \hat{x}_N^*(t_0|t_0^-)\}$. Define $\beta_{k,j} \triangleq \lambda_w(\sum_{i=j+\delta_{k+1}}^{\Delta_k+\delta_k+j-1}\lambda_x^i)$, $j = 0, \ldots, N - \Delta_k$, then for the case of $\Delta_k \leq N$, we have $\mathbb{E}\{\|\hat{x}_j^*(t_{k+1}|t_{k+1}^-) - \hat{x}_{j+\Delta_k}^*(t_k|t_k^-)\|^s|\xi(t_k), \mathcal{E}_1^k, \mathcal{E}_2^k, \mathcal{E}_1^{k+1}\} \leq \beta_{k,j}d^s$. We also define $P_{\Delta_0, \delta_1} \triangleq \mathbb{P}\{\mathcal{E}_2^0, \mathcal{E}_1^1|\mathcal{E}_1^0\}$, $R_{\delta_k} \triangleq [(1 - q_s)(1 - q_c)]^{\delta_k} - [(1 - q_s)(1 - q_c)]^{\delta_k+1}$, and $\bar{\lambda}_N \triangleq (\lambda_F\lambda_x^N + \lambda_l\sum_{i=0}^{N-1}\lambda_x^i)\lambda_w$.

We construct the following cost function, which is served as the stochastic Lyapunov function:

$$J_N(x(k)) = \sum_{j=0}^{N-1} l\left(\bar{f}^j(x(k)), u_j^*(k)\right) + F\left(\bar{f}^N(x(k))\right) \quad (36)$$

where $\bar{f}^j(x(k)) = f(\bar{f}^{j-1}(x(k)), u_{j-1}^*(k), 0)$ and $\bar{f}^0(x) = x$. We define $\xi(t_k) \triangleq [x^T(t_k^-), \boldsymbol{b}^T(t_k^-)]^T$ and it can be verified that the sequence $\{\xi(t_k)\}_{k \in \mathbb{Z}_0}$ is Markovian (Remark 8).

The main proof idea includes discussing the difference between the Lyapunov functions at two successive successful transmission instants of the control packets and analyzing the bound of the state evolution between these two instants. For ease of exposition, we divide the proof into three steps.

Step I [Values of OCF (28) at Two Consecutive Successful Transmission Instants of Control Sequences]: In this step, we discuss the upper bound of the difference $\mathbb{E}\{V_N^*(\hat{x}(t_1|t_1^-)) - V_N^*(\hat{x}(t_0|t_0^-))|\xi(t_0), \mathcal{E}_1^0, \mathcal{E}_2^0, \mathcal{E}_1^1\}$.

1) For $\Delta_0 \leq N$ case, by constructing the control sequence $\boldsymbol{u}^\#(t_1) = \{u_{\Delta_0}^*(t_0), \ldots, u_{N-1}^*(t_0), u_N^\#, \ldots, u_{N+\Delta_0-1}^\#\}$ with $u_i^\# = \kappa(\hat{x}_{i-\Delta_0}(t_1|t_1^-))$, and then following the similar lines presented in [23], we obtain $\mathbb{E}\{V_N^*(\hat{x}(t_1|t_1^-)) - V_N^*(\hat{x}(t_0|t_0^-))|\xi(t_0), \mathcal{E}_1^0, \mathcal{E}_2^0, \mathcal{E}_1^1\} \leq -l(\hat{x}(t_0|t_0^-), u_0^*(t_0)) + \Psi_0 d^s$, where $\Psi_0 = \lambda_F\beta_{0,N-\Delta_0} + \lambda_l\sum_{i=0}^{N-\Delta_0}\beta_{0,i}$.

2) For $\Delta_0 > N$ case, if $t_1^- \leq t_0 + N$, incorporating Lemma 5 and Assumption 4 yields $V_N(\hat{x}(t_1|t_1^-)) - V_N^*(\hat{x}(t_0|t_0^-)) \leq$

$\gamma^{\Delta_0 - N}F(\hat{x}(t_0 + N|t_1^-)) - V_N^*(\hat{x}(t_0|t_0^-)) \leq (\gamma^{\Delta_0 - N} - 1)F(\hat{x}_N^*(t_0|t_0^-)) - l(\hat{x}(t_0|t_0^-), u_0^*(t_0)) + \gamma^{\Delta_0 - N}[F(\hat{x}(t_0 + N|t_1^-)) - F(\hat{x}_N^*(t_0|t_0^-))]$, where $|F(\hat{x}(t_0 + N|t_1^-)) - F(\hat{x}_N^*(t_0|t_0^-))| \leq \lambda_F\beta_{0,N-\Delta_0}\|w\|^s$. Similarly, if $t_0 + N < t_1^-$, we have $V_N(\hat{x}(t_1|t_1^-)) - V_N^*(\hat{x}(t_0|t_0^-)) \leq \gamma^{\Delta_0 - N}F(x(t_0 + N)) + \sum_{j=\delta_1}^{\Delta_0 - N - 1}\gamma^j\eta\|w\|^s - V_N^*(\hat{x}(t_0|t_0^-)) \leq \gamma^{\Delta_0 - N}[F(x(t_0 + N)) - F(\hat{x}_N^*(t_0|t_0^-))] + \sum_{j=\delta_1}^{\Delta_0 - N - 1}\gamma^j\eta\|w\|^s + (\gamma^{\Delta_0 - N} - 1)F(\hat{x}_N^*(t_0|t_0^-)) - l(\hat{x}(t_0|t_0^-), u_0^*(t_0))$, where $|F(x(t_0 + N)) - F(\hat{x}_N^*(t_0|t_0^-))| \leq \lambda_F\lambda_w\sum_{j=0}^{N+\delta_0 - 1}\lambda_x^j\|w\|^s$.

It is worth noting that $\Psi_1 \triangleq \gamma^{\Delta_0 - N}\lambda_F\lambda_w\sum_{j=0}^{N+\delta_0 - 1}\lambda_x^j + \sum_{j=\delta_1}^{\Delta_0 - N - 1}\gamma^j\eta \geq \gamma^{\Delta_0 - N}\lambda_F\beta_{0,N-\Delta_0}$. Then, combining the above two inequalities and taking conditional expectation on both sides yield the following inequality:

$$\mathbb{E}\left\{V_N^*\left(\hat{x}(t_1|t_1^-)\right) - V_N^*\left(\hat{x}(t_0|t_0^-)\right)\big|\xi(t_0), \mathcal{E}_1^0, \mathcal{E}_2^0, \mathcal{E}_1^1\right\}$$
$$\leq \left(\gamma^{\Delta_0 - N} - 1\right)F\left(\hat{x}_N^*(t_0|t_0^-)\right) - l\left(\hat{x}(t_0|t_0^-), u_0^*(t_0)\right) + \Psi_1 d^s.$$

Step II (Decrement of the Lyapunov Function at Two Consecutive Successful Transmission Instants of Control Sequences): In this step, the decrement of the Lyapunov function will be analyzed separately by recognizing $J_N(x(t_1)) - J_N(x(t_0)) \leq |J_N(x(t_1)) - V_N^*(\hat{x}(t_1|t_1^-))| + V_N^*(\hat{x}(t_1|t_1^-)) - V_N^*(\hat{x}(t_0|t_0^-)) + |V_N^*(\hat{x}(t_0|t_0^-)) - J_N(x(t_0))|$.

In the following, we only deal with the $q_c \neq q_s$ case, and the case of $q_c = q_s$ can be handled similarly.

First, we obtain the inequality $\mathbb{E}\{V_N^*(\hat{x}(t_1|t_1^-)) - V_N^*(\hat{x}(t_0|t_0^-))|\xi(t_0), \mathcal{E}_1^0\} \leq \sum_{\Delta_0=1}^{N}\sum_{\delta_1=0}^{\Delta_0 - 1}P_{\Delta_0,\delta_1}[\Psi_0 d^s - l(\hat{x}(t_0|t_0^-), u_0^*(t_0))] + \sum_{\Delta_0=N+1}^{\infty}\sum_{\delta_1=0}^{\Delta_0 - 1}P_{\Delta_0,\delta_1}[(\gamma^{\Delta_0 - N} - 1)F(\hat{x}_N^*(t_0|t_0^-)) - l(\hat{x}(t_0|t_0^-), u_0^*(t_0)) + \Psi_1 d^s]$.

Notice that both $(1 - q_c)\gamma < 1$ and $(1 - q_s)\gamma < 1$ imply $(1 - q_c)(1 - q_s)\gamma < 1$. It can be easily verified that $\Psi_{\delta_0} \triangleq \sum_{\Delta_0=1}^{N}\sum_{\delta_1=0}^{\Delta_0 - 1}P_{\Delta_0,\delta_1}\Psi_0 + \sum_{\Delta_0=N+1}^{\infty}\sum_{\delta_1=0}^{\Delta_0 - 1}P_{\Delta_0,\delta_1}\Psi_1 < \infty$, and $\Lambda_N = \sum_{\Delta_0=N+1}^{\infty}\sum_{\delta_1=0}^{\Delta_0 - 1}P_{\Delta_0,\delta_1}(\gamma^{\Delta_0 - N} - 1) = [(q_s(1 - q_c)^{N+1})/(1 - (1 - q_c)\gamma) - (q_c(1 - q_s)^{N+1})/(1 - (1 - q_s)\gamma)][(\gamma - 1)/(q_s - q_c)]$, then we have

$$\mathbb{E}\{V_N^*\left(\hat{x}(t_1|t_1^-)\right) - V_N^*\left(\hat{x}(t_0|t_0^-)\right)|\xi(t_0), \mathcal{E}_1^0\}$$
$$\leq \Lambda_N F\left(\hat{x}_N^*(t_0|t_0^-)\right) - l\left(\hat{x}(t_0|t_0^-), u_0^*(t_0)\right) + \Psi_{\delta_0}d^s. \quad (37)$$

Second, by definitions of $J_N(x(t_k))$ and $V_N^*(\hat{x}(t_k|t_k^-))$, one obtains $|J_N(x(t_k)) - V_N^*(\hat{x}(t_k|t_k^-))| \leq (\lambda_l\sum_{i=0}^{N-1}\lambda_x^i + \lambda_F\lambda_x^N)\|x(t_k) - \hat{x}(t_k|t_k^-)\|^s \leq \bar{\lambda}_N\sum_{i=0}^{\delta_k - 1}\lambda_x^i\|w\|^s$. We obtain

$$\mathbb{E}\left\{\left|J_N(x(t_1)) - V_N^*\left(\hat{x}(t_1|t_1^-)\right)\right|\Big|\xi(t_0), \mathcal{E}_1^0\right\} \leq \Lambda_1 d^s \quad (38)$$

$$\mathbb{E}\left\{\left|J_N(x(t_0)) - V_N^*\left(\hat{x}(t_0|t_0^-)\right)\right|\Big|\xi(t_0), \mathcal{E}_1^0\right\} \leq \Lambda_0 d^s \quad (39)$$

where $\Lambda_0 = \bar{\lambda}_N\sum_{i=0}^{\delta_0 - 1}\lambda_x^i$ and $\Lambda_1 = \bar{\lambda}_N\sum_{\delta_1=0}^{\infty}\sum_{i=0}^{\delta_1 - 1}\lambda_x^i R_{\delta_1}$. We can verify that Λ_1 is finite as $(1 - q_s)(1 - q_c)\lambda_x < 1$.

Incorporating (37)–(39) yields

$$\mathbb{E}\left\{J_N(x(t_1)) - J_N(x(t_0))\big|\xi(t_0), \mathcal{E}_1^0\right\}$$
$$\leq \Lambda_N F\left(\hat{x}_N^*(t_0|t_0^-)\right) - l\left(\hat{x}(t_0|t_0^-), u_0^*(t_0)\right) + \Lambda_3 d^s \quad (40)$$

where $\Lambda_3 = \Lambda_0 + \Psi_{\delta_0} + \Lambda_1$.

By the definition of the conditional expectation, we obtain $\mathbb{E}\{J_N(x(t_1)) - J_N(x(t_0))|\xi(t_0)\} = \sum_{\delta_0=0}^{\infty} \mathbb{E}\{J_N(x(t_1)) - J_N(x(t_0))|\xi(t_0), \mathcal{E}_1^0\}\mathbb{P}\{\mathcal{E}_1^0\}$. Due to $(1-q_s)(1-q_c)\lambda_x < 1$, we have $\Gamma \triangleq \sum_{\delta_0=0}^{\infty} R_{\delta_0}\Lambda_3 < \infty$. $\sum_{\delta_0=0}^{\infty} R_{\delta_0}\Lambda_N = \Lambda_N$ as Λ_N does not depend on δ_0.

Since $F(\hat{x}_N^*(t_0|t_0^-)) \leq F(\hat{x}(t_0|t_0^-))$ and N is chosen such that (34) holds, we can easily verify $l(\hat{x}(t_0|t_0^-), u_0^*(t_0)) - \Lambda_N F(\hat{x}_N^*(t_0|t_0^-)) \geq \rho F(\hat{x}(t_0|t_0^-)) \geq \rho V_N^*(\hat{x}(t_0|t_0^-))$, where $\rho \triangleq -(\Lambda_N - (1+\Lambda_N)\mu) > 0$. From (39) and (40), we have $\mathbb{E}\{J_N(x(t_1)) - J_N(x(t_0))|\xi(t_0)\} \leq \Gamma d^s - \rho V_N^*(\hat{x}(t_0|t_0^-)) + \rho\mathbb{E}\{J_N(x(t_0))|\xi(t_0)\} - \rho\mathbb{E}\{J_N(x(t_0))|\xi(t_0)\} \leq \bar{\Gamma} d^s - \rho\mathbb{E}\{J_N(x(t_0))|\xi(t_0)\}$, where $\bar{\Gamma} = \sum_{\delta_0=0}^{\infty} R_{\delta_0}\bar{\lambda}_N \sum_{i=0}^{\delta_0-1} \lambda_x^i + \Gamma < \infty$. Then, it yields

$$\mathbb{E}\{J_N(x(t_1))|\xi(t_0)\} \leq (1-\rho)\mathbb{E}\{J_N(x(t_0))|\xi(t_0)\} + \bar{\Gamma} d^s. \quad (41)$$

Step III (Stochastic Stability): In this step, we conclude the proof based on the previous results. For the state during time interval (t_0, t_1), we have the following inequalities by the similar method in [21], [23]:

$$\sum_{j=0}^{\Delta_0-1} \mathbb{E}\{\|x(t_0+j)\|^s|\xi(t_0), \mathcal{E}_1^0\}$$
$$\leq \sum_{i=N}^{\infty} Q_i \sum_{j=N}^{i} \mathbb{E}\{\|x(t_0+j)\|^s|\xi(t_0), \mathcal{E}_1^0, \Delta_0 = i\}$$
$$+ \sum_{j=0}^{N-1} \mathbb{E}\{\|x(t_0+j)\|^s|\xi(t_0), \mathcal{E}_1^0, \Delta_0 = N\} \quad (42)$$

where $Q_i = [(q_s q_c)/(q_s - q_c)][(1-q_c)^i - (1-q_s)^i]$.

On the one hand, according to the inequality $|a+b|^s \leq 2^s(|a|^s + |b|^s)$, we obtain

$$\sum_{j=0}^{N-1} \mathbb{E}\{\|x(t_0+j)\|^s|\xi(t_0), \mathcal{E}_1^0, \Delta_0 = N\}$$
$$\leq 2^s \sum_{j=0}^{N-1} \mathbb{E}\{\|x(t_0+j) - \hat{x}_j(t_0|t_0^-)\|^s|\xi(t_0), \mathcal{E}_1^0, \Delta_0 = N\}$$
$$+ 2^s \sum_{j=0}^{N-1} \mathbb{E}\{\|\hat{x}_j(t_0|t_0^-)\|^s|\xi(t_0), \mathcal{E}_1^0, \Delta_0 = N\}$$
$$\leq \frac{2^s}{\alpha_l} \mathbb{E}\{J_N(x(t_0))|\xi(t_0), \mathcal{E}_1^0\} + C_1 d^s$$
$$+ \frac{2^s}{\alpha_l} \mathbb{E}\{|V_N^*(\hat{x}(t_0|t_0^-)) - J_N(x(t_0))||\xi(t_0), \mathcal{E}_1^0\}$$
$$\leq \frac{2^s}{\alpha_l} \mathbb{E}\{J_N(x(t_0))|\xi(t_0), \mathcal{E}_1^0\} + C_2 d^s \quad (43)$$

where $C_1 = 2^s \lambda_w \sum_{j=0}^{N-1} \sum_{i=0}^{j+\delta_0-1} \lambda_x^i$ and $C_2 = C_1 + \Lambda_0$. The third inequality is the direct result of (39).

On the other hand, incorporating with Assumption 3 gives

$$\sum_{j=N}^{i} \mathbb{E}\{\|x(t_0+j)\|^s|\xi(t_0), \mathcal{E}_1^0, \Delta_0 = i\}$$
$$\leq \frac{1}{\alpha_F} \sum_{j=N}^{i} \gamma^{j-N} \mathbb{E}\{F(x(t_0+N))|\xi(t_0), \mathcal{E}_1^0\} + C_4 d^s$$
$$\leq C_3 \mathbb{E}\{F(x(t_0+N)) - F(\hat{x}_N(t_0|t_0^-)) + V_N^*(\hat{x}(t_0|t_0^-))$$
$$- J_N(x(t_0)) + J_N(x(t_0))|\xi(t_0), \mathcal{E}_1^0\} + C_4 d^s$$

$$\leq C_3 \mathbb{E}\{J_N(x(t_0))|\xi(t_0), \mathcal{E}_1^0\} + C_5 d^s \quad (44)$$

where $C_3 = [(1-\gamma^{i-N+1})/(\alpha_F(1-\gamma))]$, $C_4 = (\eta/\alpha_F)[[(i-N+1)/(1-\gamma)] - [(1-\gamma^{i-N+1})/((1-\gamma)^2)]]$, and $C_5 = C_4 + \Lambda_0 + \lambda_F \lambda_w \sum_{i=0}^{N+\delta_0-1} \lambda_x^i$. Substituting (43) and (44) into (42) gives

$$\sum_{j=0}^{\Delta_0-1} \mathbb{E}\{\|x(t_0+j)\|^s|\xi(t_0)\}$$
$$\leq \sum_{\delta_0=0}^{\infty} \mathbb{P}\{\mathcal{E}_1^0\}\left[C_6 \mathbb{E}\{J_N(x(t_0))|\xi(t_0), \mathcal{E}_1^0\} + C_7 d^s\right]$$
$$= C_6 \mathbb{E}\{J_N(x(t_0))|\xi(t_0)\} + C_8 d^s \quad (45)$$

where $C_6 = [2^s/\alpha_l] + \sum_{i=N}^{\infty} Q_i C_3$, $C_7 = C_2 + \sum_{i=N}^{\infty} Q_i C_5$, and $C_8 = \sum_{\delta_0=0}^{\infty} R_{\delta_0} C_7$.

Based on the Markov property of $\{\xi(t_k)\}_{k \in \mathbb{Z}_0}$, (41) can be directly extended to any time $t_k \ \forall k \in \mathbb{Z}_0$, then we have $\mathbb{E}\{J_N(x(t_k))|\xi(t_0)\} \leq (1-\rho)^k \mathbb{E}\{J_N(x(t_0))|\xi(t_0)\} + \bar{\Gamma}[(1-(1-\rho)^k)/\rho]d^s$. Similarly, (45) can also be extended to $\sum_{j=0}^{\Delta_k-1} \mathbb{E}\{\|x(t_k+j)\|^s|\xi(t_0)\} \leq C_6 \mathbb{E}\{J_N(x(t_k))|\xi(t_0)\} + C_8 d^s$. Therefore, we can conclude that $\sum_{j=0}^{\Delta_k-1} \mathbb{E}\{\|x(t_k+j)\|^s|\xi(t_0)\} \leq C_6(1-\rho)^k \mathbb{E}\{J_N(x(t_0)) - V_N^*(\hat{x}(t_0|t_0^-)) + F(\hat{x}(t_0|t_0^-))|\xi(t_0)\} + (C_6 C_0/\rho + C_8)d^s \leq C_{10}(1-\rho)^k \mathbb{E}\{\|\hat{x}(t_0|t_0^-) - x(t_0) + x(t_0)\|^s|\xi(t_0)\} + C_9 d^s \leq 2^s C_{10}(1-\rho)^k \mathbb{E}\{\|x(t_0)\|^s|\xi(t_0)\} + C_{11}d^s$, where $C_{10} = \lambda_F C_6$, $C_9 = \sum_{\delta_0=0}^{\infty} \bar{\lambda}_N \sum_{i=0}^{\delta_0-1} \lambda_x^i C_6 + C_6 C_0/\rho + C_8$, and $C_{11} = C_9 + 2^s C_{10} \sum_{\delta_0=0}^{\infty} \lambda_w \sum_{i=0}^{\delta_0-1} \lambda_x^i R_{\delta_0}$.

As mentioned before, the inputs during $[0, t_0 - 1]$ are 0. Based on Assumption 3 and the fact that $\mathbb{P}\{t_0 = \vartheta\} = q_c(1-q_c)^{\vartheta}$, we obtain $\sum_{j=0}^{\Delta_k-1} \mathbb{E}\{\mathbb{E}\{\|x(t_k+j)\|^s|\xi(t_0)\}|\xi_0\} = \sum_{j=0}^{\Delta_k-1} \mathbb{E}\{\|x(t_k+j)\|^s|\xi_0\} \leq C_{11}d^s + 2^s C_{10}(1-\rho)^k \mathbb{E}\{\|x(t_0)\|^s|\xi_0\} \leq 2^s C_{10}/\alpha_F(1-\rho)^k \sum_{\vartheta=0}^{\infty} q_c(1-q_c)^{\vartheta} \times \mathbb{E}\{F(x(\vartheta))|\xi_0\} + C_{11}d^s \leq 2^s C_{10}/\alpha_F(1-\rho)^k \sum_{\vartheta=0}^{\infty} q_c(1-q_c)^{\vartheta}\gamma^{\vartheta}F(x_0) + c_2 d^s \leq c_1(1-\rho)^k\|x_0\|^s + c_2 d^s$, where $\xi_0 = [x_0^T \ \boldsymbol{b}(0)^T]^T$, $c_1 = 2^s C_{10}\lambda_F q_c/\alpha_F \sum_{\vartheta=0}^{\infty}(1-q_c)^{\vartheta}\gamma^{\vartheta}$, and $c_2 = C_{11} + 2^s C_{10}\eta q_c/\alpha_F(1-\gamma)\sum_{\vartheta=0}^{\infty}(1-q_c)^{\vartheta}(1-\gamma^{\vartheta})$.

For $k \in [0, t_0 - 1]$, the upper bound of $\mathbb{E}\{\|x(k)\|^s\}$ can be similarly obtained. These complete the proof. ∎

The above theorem reveals the dependence of the stability of each system on three parameters: N, q_s, and q_c. The SAP demands $\bar{q}_s$ and $\bar{q}_c$ can then be selected accordingly.

From the proof of Theorem 3, we claim that *if the system is stable with prediction horizon N and SAP demands $\bar{q}_s$ and $\bar{q}_c$, then the system with SAPs satisfying $q_s \geq \bar{q}_s$ and $q_c \geq \bar{q}_c$ is also stable.* With this claim, the stability can be guaranteed under the dual scheduling strategy. To be specific, for the access strategy of sensors, if the NEP is achieved, the SAP keeps unchangeable; otherwise, the SAP converges to $\bar{q}_s$ (Theorem 1). In general, this convergence process is negligible as the NEP can be achieved fairly fast by (17) or (18). For the scheduling strategy of the central scheduler, we have $q_c \geq \bar{q}_c$ although q_c may be time varying.

Remark 8: Different from the proof in [23, Th. 1], the sequences $\{x(t_k)\}_{k \in \mathbb{Z}_0}$, $\{x(t_k^-)\}_{k \in \mathbb{Z}_0}$, and $\{\hat{x}(t_k|t_k^-)\}_{k \in \mathbb{Z}_0}$ in our settings are non-Markovian, thus challenging the stability analysis. To address this challenge, we construct an extended state sequence $\{\xi(t_k)\}_{k \in \mathbb{Z}_0}$ with $\xi(t_k) = [x^T(t_k^-), \boldsymbol{b}^T(t_k^-)]^T$, which is

Markovian as $\xi(t_{k+1})$ depends entirely on the state $\xi(t_k)$ and is conditionally independent of the history.

Remark 9: For the one-channel packet losses case (e.g., only control channel is considered) studied in [21] and [23], a result similar to (34) was developed, that is, $[((1 - q_c)^N(\gamma - 1))/(1 - (1 - q_c)\gamma)] < \mu/(1 - \mu)$. In fact, this inequality is equivalent to (34) with $q_s = 1$, and thus can be treated as a special case of our result.

Remark 10: The usage of PBMPC relaxes the requirement of SAPs. Taking a scalar LTI system subject to i.i.d. packet losses, for example, a necessary and sufficient condition for mean square stabilizability is $(1 - q_s q_c)|a| < 1$ (a is the system pole, and $q_s q_c$ is the equivalent SAP) [35]. But this condition is weakened to $(1 - \min\{q_s, q_c\})|a| < 1$ (Assumption 3) by properly choosing N to satisfy (34).

V. NUMERICAL SIMULATIONS

For the ease of presentation and without loss of generality, we consider four scalar open-loop unstable nonlinear systems to show the effectiveness of the proposed dual scheduling strategy under the PBMPC framework

$$x_i(k + 1) = x_i(k) + a_i \sin(x_i(k)/5) + u_i(k) + w_i(k) \quad (46)$$

where $a_1 = 1.0$, $a_2 = 0.4$, $a_3 = 0.2$, $a_4 = 0.6$, $w_i \in [-0.1, 0.1]$ is the bounded random disturbance, and $u_i(k)$ is the control input with constraint $|u_i(k)| \leq 2.0$. Suppose that system 1, system 2, and system 3 begin to operate at time $k = 0$, system 2 leaves the channel at time $k = 1000$, and a new system 4 joins the channel at time $k = 2000$. The initial states are $x_1(0) = x_2(0) = 10$ and $x_3(0) = x_4(2000) = -10$.

Suppose that the measurement and control channels are modeled as block-fading additive white Gaussian noise channels and the digital communication uses binary-phase shift keying transmission. The PRP $P_i(h)$ [including $P_{si}(h)$ and $P_{ci}(h)$] then takes the following form [28]:

$$P_i(h) = \left(\int_{-\infty}^{\sqrt{h\zeta_i}} \frac{1}{\sqrt{2\pi}} e^{-t^2/2} dt \right)^{b_i}. \quad (47)$$

The local channel gain denoted by h_{si} is available to each sensor i and the full channel gains $\{h_{ci}, i = 1, 2, 3, 4\}$ are also available to the central scheduler. We also assume that h_{si} and h_{ci} follow the exponential distribution with parameters $\lambda_{s1} = \lambda_{c1} = 0.8$, $\lambda_{s2} = \lambda_{c2} = 1.2$, $\lambda_{s3} = \lambda_{c3} = 1.8$, and $\lambda_{s4} = \lambda_{c4} = 1.0$. The packet length of state packet is $b_{si} = 8$ bits and control packet is $b_{ci} = 8 \times N_i$ bits, where N_i is the prediction horizon of system i that needs to be determined. The transmit powers for each sensor and controller are given by $\zeta_{si} = 25$ and $\zeta_{ci} = 40$, $i = 1, 2, 3, 4$.

For the design of control scheme, we choose the stage cost function and the terminal cost function as $l_i(x) = \|x\|$ and $F_i(x) = 2\|x\|$, and then Assumptions 2 and 3 can be satisfied with $\alpha_{Fi} = \lambda_{Fi} = 2$, $\lambda_{wi} = \lambda_{li} = \alpha_{li} = s = 1$, and $\lambda_{xi} = 1 + a_i/5$. Assumption 4 is satisfied with the terminal controller $\kappa_i(x) = -a_i \sin(x/5) - x(2 - a_i)/(|x_i(t_0)| + 20)$ and Assumption 5 holds with $\gamma_i = 1 + a_i/5$ and $\eta_i = 1$.

We first determine the SAP demands for each system such that $(1 - \bar{q}_{si})\gamma_i < 1$. Specifically, let $\bar{q}_{s1} = 0.2$, $\bar{q}_{s2} = 0.11$,
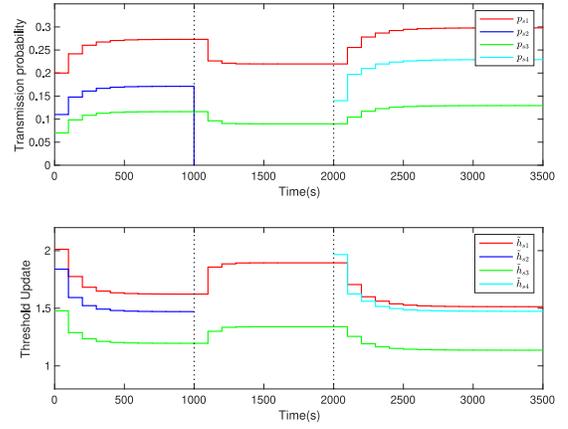
Fig. 4. Update of access probability $p_{si}(k)$ for each sensor computed by the best-response dynamic (17) or better-response dynamic (18) with $\beta = 0$, and the update of the realted threshold level $\tilde{h}_{si}(k)$ of the access strategy.
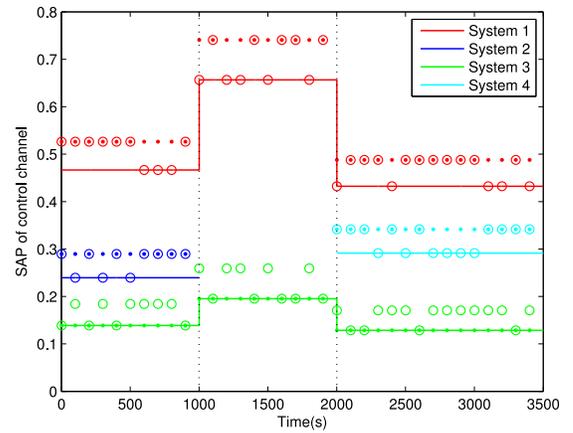
Fig. 5. Comparison of the SAPs obtained by i.i.d. scheduling (solid lines), threshold strategy with fixed priority (solid points), and threshold strategy with random priority (empty circles).

$\bar{q}_{s3} = 0.07$, $\bar{q}_{s4} = 0.14$, and $\bar{q}_{ci}$ ($i = 1, \ldots, n$) are selected a bit larger than $\bar{q}_{si}$, then the inequalities $(1 - \bar{q}_{si})(1 - \bar{q}_{ci})\lambda_{xi} < 1$ and (34) are satisfied with $N_1 = 10$ and $N_2 = N_3 = N_4 = 12$. From Theorem 3, the stability of each system is guaranteed.

The simulation results are illustrated in Figs. 4–7.

1) The strategy update mechanism (17) or (18) with initial access probabilities $p_{si}^0 = \bar{q}_{si}$ ($i = 1, 2, 3, 4$) is performed every 100 time slots ($M = 100$), and the simulation results are shown in Fig. 4. We observe that the access probabilities quickly converge to NEP. Note that the access probability is not large and the corresponding threshold is large such that PRPs $P_{si}(\tilde{h}_{si})$ are very close to 1. This leads to $H_i(p_{si}) = p_{si} = H_i^{-1}(p_{si})$ and in turn yields the equivalence between the best-response dynamic (17) and better-response dynamic (18) with $\beta = 0$. The threshold of the access strategy $\tilde{h}_{si}(k)$ is also shown in Fig. 4. Because of the exponential distribution and $p_{si} = \int_{\tilde{h}_{si}}^{\infty} o_{si}(h)dh$, the analytical expression of $\tilde{h}_{si}$ can be written as $\tilde{h}_{si} = -\ln(p_{si})/\lambda_{si}$.

2) Given the access probability of each controller by (20), we make a comparison of SAPs obtained by i.i.d.
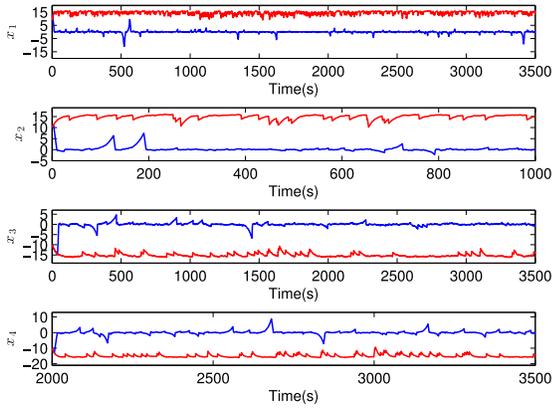
Fig. 6. State responses with packet-based compensation. The blue line is obtained by PBMPC and the red line is obtained without active compensation.
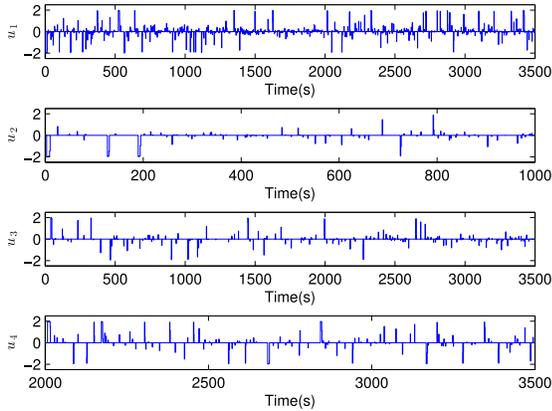
Fig. 7. Actual control input with packet-based control compensation.

strategy (21), threshold strategy with fixed priority, and threshold strategy with random priority. It can be observed that the threshold strategy with fixed priority is superior to the i.i.d. scheduling expect for the system with minimum priority, whose SAP can be increased to some extent by the threshold strategy with random priority.

3) Figs. 6 and 7 show the state responses and the actual control inputs of the four systems based on the distributed access mechanism for each sensor, threshold strategy with random priority for each controller, and PBMPC algorithm. We observe that all systems are stable and the control constraints are all satisfied.

4) To show the superiority of the PBMPC scheme, we conduct a comparison simulation where the auxiliary control law $\kappa_i(x)$ is applied in the absence of any control compensation. The results are shown in Fig. 6. All states of the four systems do not approach to the origin. Indeed, the equivalent packet loss probabilities are high $(1 - q_{si}q_{ci}, i = 1, \ldots, 4)$, and all systems operate for a long time in an open-loop manner.

VI. Conclusion

The scheduling and control of wireless cloud control systems are investigated, where multiple control systems are

involved. A dual scheduling strategy is proposed under the PBMPC framework. It is shown that the channel-aware threshold scheduling strategy is optimal for each sensor, which guarantees efficient NEP. The stability of the control systems can be ensured by choosing the appropriate prediction horizon and the SAP demands of sensors and controllers.

Appendix A
Properties of $H_i(p_{si})$

Lemma 7: Consider the function $H_i(p_{si})$ defined in (14), we have the following facts.

1) $H_i(p_{si})$ is a continuous, strictly increasing, and concave function with $H_i(0) = 0$.
2) $H_i(p_{si}) = \int_0^{p_{si}} P_{si}(\tilde{h}_{si}(p))dp$.
3) $H_i(p_{si}) \leq p_{si} \leq H_i^{-1}(p_{si})$.
4) $p_{si}/H_i(p_{si})$ is an increasing function with respect to p_{si}.

Proof:

1) Denote $\tilde{h}_{si}^{-1}(.)$ as the inverse function of $\tilde{h}_{si}(.)$ and $\tilde{h}_{si}^{-1}(\infty) = 0$. Let $p = \tilde{h}_{si}^{-1}(h)$, then (14) can be rewritten as $H_i(p_{si}) = -\int_0^{p_{si}} o_{si}(\tilde{h}_{si}(p)) P_{si}(\tilde{h}_{si}(p))[(d\tilde{h}_{si}(p))/dp]dp$, where $[(d\tilde{h}_{si}(p))/dp] = -1/o_{si}(\tilde{h}_{si}(p))$. Obviously, we have $H_i(0) = 0$. Differentiating both side with respect to p_{si} yields $H_i'(p_{si}) = P_{si}(\tilde{h}_{si}(p_{si})) > 0$, which implies that $H_i(p_{si})$ is a strictly increasing function. Furthermore, $P_{si}(\tilde{h}_{si}(p_{si}))$ is a decreasing function with respect to p_{si}, that is, $H_i(p_{si})$ is concave.
2) Making a change of variable by means of a substitution $h = \tilde{h}_{si}(p)$ obtains the result directly.
3) From 1), we see that $H_i(p_{si}) \leq p_{si}$ since $P_{si}(\tilde{h}_{si}(p)) \leq 1$. As shown previously, H_i is a strictly increasing continuous function, so is its inverse function H_i^{-1}. Hence, it follows that $H_i^{-1}(H_i(p_{si})) \leq H_i^{-1}(p_{si})$, that is, $p_{si} \leq H_i^{-1}(p_{si})$.
4) Taking the differentiation with respect to p_{si}, we have $(p_{si}/[H_i(p_{si})])' = [(\int_0^{p_{si}} P_{si}(\tilde{h}_{si}(p)) - P_{si}(\tilde{h}_{si}(p_{si}))dp)/(H_i^2(p_{si}))] \geq 0$. This inequality holds because $P_{si}(\tilde{h}_{si}(p))$ is decreasing with respect to p. ∎

Appendix B
Proof of Lemma 1

Assume by the way of contradiction that the strategy profile π_s^* is a best-response strategy but not the threshold strategy. That is, there exists an index i such that $\pi_{si}^*(h)$ is not a threshold strategy. For sensor i, the access probability $p_{si} = \int_0^\infty \pi_{si}^*(h)o_{si}(h)dh$ achieves the minimum, and the constraint $\int_0^\infty \pi_{si}^*(h)o_{si}(h)P_{si}(h)dh \prod_{j \neq i}(1 - p_{sj}) \geq \bar{q}_{si}$ is met.

We construct a new strategy profile $(z_{si}(\tilde{h}_{si}), \pi_{-si}^*)$, where $z_{si}(\tilde{h}_{si})$ is a threshold strategy with the threshold $\tilde{h}_{si}$ determined by the following equation:

$$\int_{\tilde{h}_{si}}^\infty o_{si}(h)P_{si}(h)dh = \int_0^\infty \pi_{si}^*(h)o_{si}(h)P_{si}(h)dh \quad (48)$$

where $\tilde{h}_{si}$ always exists since the right-hand side of (48) is not greater than $\int_0^\infty o_{si}(h)P_{si}(h)dh$.

As π_{si}^* is not a threshold strategy, we have $\pi_{si}^*(h) \leq 1$. Due to the fact that $P_{si}(h)$ is a strictly increasing function, we have

$$\int_0^{\tilde{h}_{si}} \pi_{si}^*(h) o_{si}(h)\left(P_{si}(h) - P_{si}\left(\tilde{h}_{si}\right)\right) dh < 0$$

$$\int_{\tilde{h}_{si}}^{\infty} \left(1 - \pi_{si}^*(h)\right) o_{si}(h)\left(P_{si}\left(\tilde{h}_{si}\right) - P_{si}(h)\right) dh < 0.$$

Then, (48) implies that $\int_{\tilde{h}_{si}}^{\infty} o_{si}(h) dh - \int_0^{\infty} \pi_{si}^*(h) o_{si}(h) dh = [1/(P_{si}(\tilde{h}_{si}))] [\int_{\tilde{h}_{si}}^{\infty} (1 - \pi_{si}^*(h)) o_{si}(h) P_{si}(\tilde{h}_{si}) dh - \int_0^{\tilde{h}_{si}} \pi_{si}^*(h) o_{si}(h) \times P_{si}(\tilde{h}_{si}) dh] < [1/(P_{si}(\tilde{h}_{si}))] [\int_{\tilde{h}_{si}}^{\infty} (1 - \pi_{si}^*(h)) o_{si}(h) P_{si}(h) dh - \int_0^{\tilde{h}_{si}} \pi_{si}^*(h) o_{si}(h) P_{si}(h) dh] = 0$. This equation means that $z_{si}(\tilde{h}_{si})$ is a lower cost strategy, and thus contradicts the optimality of $\boldsymbol{\pi}_s^*$.

REFERENCES

[1] P. Park, S. C. Ergen, C. Fischione, C. Lu, and K. H. Johansson, "Wireless network design for control systems: A survey," *IEEE Commun. Surveys Tuts.*, vol. 20, no. 2, pp. 978–1013, 2nd Quart., 2018.

[2] Y. Xia, "Cloud control systems," *IEEE/CAA J. Automatica Sinica*, vol. 2, no. 2, pp. 134–142, Apr. 2015.

[3] G.-P. Liu, "Predictive control of networked multiagent systems via cloud computing," *IEEE Trans. Cybern.*, vol. 47, no. 8, pp. 1852–1859, Aug. 2017.

[4] M. Mozaffari, W. Saad, M. Bennis, and M. Debbah, "Mobile unmanned aerial vehicles (uavs) for energy-efficient Internet of Things communications," *IEEE Trans. Wireless Commun.*, vol. 16, no. 11, pp. 7574–7589, Nov. 2017.

[5] J. J. Leonard and A. Bahr, "Autonomous underwater vehicle navigation," in *Springer Handbook of Ocean Engineering*. Cham, Switzerland: Springer, 2016, pp. 341–358.

[6] X. Ge, F. Yang, and Q.-L. Han, "Distributed networked control systems: A brief overview," *Inf. Sci.*, vol. 380, pp. 117–131, Feb. 2017.

[7] S.-L. Dai, H. Lin, and S. S. Ge, "Scheduling-and-control codesign for a collection of networked control systems with uncertain delays," *IEEE Trans. Control Syst. Technol.*, vol. 18, no. 1, pp. 66–78, Jan. 2010.

[8] B. Shen, Z. Wang, D. Wang, and H. Liu, "Distributed state-saturated recursive filtering over sensor networks under round-robin protocol," *IEEE Trans. Cybern.*, vol. 50, no. 8, pp. 3605–3615, Aug. 2020, doi: 10.1109/TCYB.2019.2932460.

[9] K. Liu, E. Fridman, and K. H. Johansson, "Networked control with stochastic scheduling," *IEEE Trans. Autom. Control*, vol. 60, no. 11, pp. 3071–3076, Nov. 2015.

[10] S. Al-Areqi, D. Görges, and S. Liu, "Event-based networked control and scheduling codesign with guaranteed performance," *Automatica*, vol. 57, pp. 128–134, Jul. 2015.

[11] K. Gatsis, M. Pajic, A. Ribeiro, and G. J. Pappas, "Opportunistic control over shared wireless channels," *IEEE Trans. Autom. Control*, vol. 60, no. 12, pp. 3140–3155, Dec. 2015.

[12] E. Henriksson, D. E. Quevedo, E. G. Peters, H. Sandberg, and K. H. Johansson, "Multiple-loop self-triggered model predictive control for network scheduling and control," *IEEE Trans. Control Syst. Technol.*, vol. 23, no. 6, pp. 2167–2181, Nov. 2015.

[13] M. Kögel and R. Findeisen, "Combined online communication scheduling and output feedback MPC of cyber-physical systems," in *Proc.16th IEEE Annu. Consum. Commun. Netw. Conf.*, 2019, pp. 1–6.

[14] L. Lyu, C. Chen, C. Hua, S. Zhu, and X. Guan, "Co-design of stabilisation and transmission scheduling for wireless control systems," *IET Control Theory Appl.*, vol. 11, no. 11, pp. 1767–1778, Jul. 2017.

[15] A. Molin and S. Hirche, "Price-based adaptive scheduling in multi-loop control systems with resource constraints," *IEEE Trans. Autom. Control*, vol. 59, no. 12, pp. 3282–3295, Dec. 2014.

[16] K. Gatsis, A. Ribeiro, and G. J. Pappas, "Random access design for wireless control systems," *Automatica*, vol. 91, pp. 1–9, May 2018.

[17] M. Calvo-Fullana, C. Antón-Haro, J. Matamoros, and A. Ribeiro. (2018). *Random Access Communication for Wireless Control Systems With Energy Harvesting Sensors*. [Online]. Available: https://arxiv.org/abs/1801.10141

[18] Y.-B. Zhao, G. P. Liu, Y. Kang, and L. Yu, *Packet-Based Control for Networked Control Systems*. Singapore: Springer, 2018.

[19] X. Tang, L. Deng, N. Liu, and S. Yang, "Observer-based output feedback MPC for T–S fuzzy system with data loss and bounded disturbance," *IEEE Trans. Cybern.*, vol. 49, no. 6, pp. 2119–2132, Jun. 2019.

[20] D. E. Quevedo and D. Nešić, "Input-to-state stability of packetized predictive control over unreliable networks affected by packet-dropouts," *IEEE Trans. Autom. Control*, vol. 56, no. 2, pp. 370–375, Feb. 2011.

[21] Y. Long, S. Liu, and L. Xie, "Stochastic channel allocation for networked control systems," *IEEE Control Syst. Lett.*, vol. 1, no. 1, pp. 176–181, Jul. 2017.

[22] H. Yang, H. Zhao, Y. Xia, and J. Zhang, "Event-triggered active MPC for nonlinear multiagent systems with packet losses," *IEEE Trans. Cybern.*, early access, Apr. 17, 2019, doi: 10.1109/TCYB.2019.2908389.

[23] D. E. Quevedo and D. Nešić, "Robust stability of packetized predictive control of nonlinear systems with disturbances and Markovian packet losses," *Automatica*, vol. 48, no. 8, pp. 1803–1811, 2012.

[24] C. Liu, J. Gao, H. Li, and D. Xu, "Aperiodic robust model predictive control for constrained continuous-time nonlinear systems: An event-triggered approach," *IEEE Trans. Cybern.*, vol. 48, no. 5, pp. 1397–1405, May 2018.

[25] H. Li and Y. Shi, "Network-based predictive control for constrained nonlinear systems with two-channel packet dropouts," *IEEE Trans. Ind. Electron.*, vol. 61, no. 3, pp. 1574–1582, Mar. 2014.

[26] L. Zou, Z. Wang, Q.-L. Han, and D. Zhou, "Ultimate boundedness control for networked systems with try-once-discard protocol and uniform quantization effects," *IEEE Trans. Autom. Control*, vol. 62, no. 12, pp. 6582–6588, Dec. 2017.

[27] P. Li, Y. Kang, Y.-B. Zhao, and Z. Yuan, "Packet-based model predictive control for networked control systems with random packet losses," in *Proc. 57th IEEE Conf. Decis. Control*, 2018, pp. 3457–3462.

[28] A. S. Leong and D. E. Quevedo, "Kalman filtering with relays over wireless fading channels," *IEEE Trans. Autom. Control*, vol. 61, no. 6, pp. 1643–1648, Jun. 2016.

[29] I. Menache and N. Shimkin, "Rate-based equilibria in collision channels with fading," *IEEE J. Sel. Areas Commun.*, vol. 26, no. 7, pp. 1070–1077, Sep. 2008.

[30] K. Gatsis, A. Ribeiro, and G. J. Pappas, "Optimal power management in wireless control systems," *IEEE Trans. Autom. Control*, vol. 59, no. 6, pp. 1495–1510, Jun. 2014.

[31] B. Yang, Y. Shen, M. Johansson, C. Chen, and X. Guan, "Opportunistic multichannel access with decentralized channel state information," *Wireless Commun. Mobile Comput.*, vol. 15, no. 2, pp. 322–339, 2015.

[32] L. Chen, S. H. Low, and J. C. Doyle, "Random access game and medium access control design," *IEEE/ACM Trans. Netw.*, vol. 18, no. 4, pp. 1303–1316, Aug. 2010.

[33] K. Cohen, A. Leshem, and E. Zehavi, "Game theoretic aspects of the multi-channel aloha protocol in cognitive radio networks," *IEEE J. Sel. Areas Commun.*, vol. 31, no. 11, pp. 2276–2288, Nov. 2013.

[34] I. Menache and N. Shimkin, "Reservation-based distributed medium access in wireless collision channels," *Telecommun. Syst.*, vol. 47, no. 1-2, pp. 95–108, 2011.

[35] H. Ishii, "Limitations in remote stabilization over unreliable channels without acknowledgements," *Automatica*, vol. 45, no. 10, pp. 2278–2285, 2009.
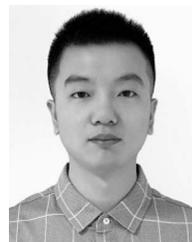
Pengfei Li (Member, IEEE) received the Ph.D. degree in control science and engineering from the University of Science and Technology of China (USTC), Hefei, China, in 2020.

He is currently a Postdoctoral Fellow with the School of Information Science and Technology, USTC. His research interests include networked control systems, model predictive control, and learning-based control.

Yun-Bo Zhao (Senior Member, IEEE) received the B.Sc. degree from Shandong University, Jinan, China, in 2003, the M.Sc. degree from the Key Laboratory of Systems and Control, Chinese Academy of Sciences, Beijing, China, in 2007, and the Ph.D. degree from the University of Glamorgan, Pontypridd, U.K., in 2008.

He is currently a Professor with the University of Science and Technology of China, Hefei, China. He had worked with INRIA, Grenoble, France; the University of Glasgow, Glasgow, U.K.; and Imperial College London, London, U.K., on various research projects. His main research interests include networked control systems, AI-enabled control, human–machine integrated intelligence, and systems biology.

Yu Kang (Senior Member, IEEE) received the Ph.D. degree in control theory and control engineering from the University of Science and Technology of China, Hefei, China, in 2005.

From 2005 to 2007, he was a Postdoctoral Fellow with the Academy of Mathematics and Systems Science, Chinese Academy of Sciences, Beijing, China. He is currently a Professor with the State Key Laboratory of Fire Science, Department of Automation, and the Institute of Advanced Technology, University of Science and Technology of China, and with the Key Laboratory of Technology in GeoSpatial Information Processing and Application System, Chinese Academy of Sciences. His current research interests include monitoring of vehicle emissions, adaptive/robust control, variable structure control, mobile manipulator, and Markovian jump systems.